MECHANISMS AND PATHWAYS OF INOSITOL PHOSPHATE DEGRADATION: EVIDENCE FROM PHOSPHATE OXYGEN STABLE ISOTOPE RATIOS AND ^{31}P NUCLEAR MAGNETIC RESONANCE SPECTROSCOPY

by

Jiangqi Wu

A thesis submitted to the Faculty of the University of Delaware in partial fulfillment of the requirements for the degree of Master of Science in Plant and Soil Sciences

Summer 2014

© 2014 Jiangqi Wu
All Rights Reserved

UMI Number: 1567834

All rights reserved

INFORMATION TO ALL USERS
The quality of this reproduction is dependent upon the quality of the copy submitted.

In the unlikely event that the author did not send a complete manuscript
and there are missing pages, these will be noted. Also, if material had to be removed,
a note will indicate the deletion.

UMI 1567834

Published by ProQuest LLC (2014). Copyright in the Dissertation held by the Author.

Microform Edition © ProQuest LLC.
All rights reserved. This work is protected against
unauthorized copying under Title 17, United States Code

ProQuest LLC.
789 East Eisenhower Parkway
P.O. Box 1346
Ann Arbor, MI 48106 - 1346

MECHANISMS AND PATHWAYS OF INOSITOL PHOSPHATE DEGRADATION: EVIDENCE FROM PHOSPHATE OXYGEN STABLE ISOTOPE RATIOS AND ^{31}P NUCLEAR MAGNETIC RESONANCE SPECTROSCOPY

by

Jiangqi Wu

Approved: _____
Dr. Deb Jaisi, Ph.D.
Professor in charge of thesis on behalf of the Advisory Committee

Approved: _____
Blake C. Meyers, Ph.D.
Chair of the Department of Plant and Soil Sciences

Approved: _____
Mark Rieger, Ph.D.
Dean of the College of Agriculture and Natural Resources

Approved: _____
James G. Richards, Ph.D.
Vice Provost for Graduate and Professional Education

ACKNOWLEDGMENTS

I would like to express my sincere appreciation to many people who have helped and encouraged me during my last two years at the University of Delaware.

My foremost thanks goes to my advisor, Dr. Deb Jaisi for his extraordinary guidance and dedication. His constant support, encouragement, and patience accompanied me throughout the past two years has greatly helped me accomplish my research and shape my research skills. I also would like to acknowledge my thesis committee members, Dr. Donald Sparks and Dr. Amy Shober for all their suggestions and cooperation.

I would like to express my enormous thank you to the help and support from my coworkers in the Environmental Biogeochemistry research group. I am particularly grateful to Prajwal Paudel for his valuable assistance on NMR data analysis and Lisa Stout for her generous help on my bacterial and enzymatic experiments. I also owe a thank you to Sunendra Raj Joshi for his great help on oxygen isotope measurement. Big thank you to Xiaona Li and Wei Li for their sincere encouragement and suggestion for my research. Thanks to Hui Li for her help and support as a great friend. Thanks to Kiran Upreti for her warmhearted help and encouragement. Thanks to Yu-sung Wu for her great help on the enzyme purification work. Special thanks to the Soil Testing Lab, in particular, Catherine Olsen and Karen Gartley for their valuable work. Additionally, I would like to extend tremendous thanks to my close friends for their encouragement and support throughout this journey.

Finally, my deepest gratitude goes to my precious family. I could never have made it through this process without their unconditioned love and encouragement.

TABLE OF CONTENTS

LIST OF TABLES

LIST OF FIGURES

ABSTRACT

Phytate and its partially dephosphorylated products exist in soils as well as in aquatic systems, but the origins, chemical forms, bioavailability and mobility of these compounds are not well understood. With increasing phytate P in agricultural soils due to manure application and consequential increase in environmental concern due to elevated P in many open waters, new methods that have higher specificity to elucidate the mechanisms and pathways of phytate degradation as well as capability for tracking sources of dissolved P are required. Application of any stable isotopes to understand inositol phosphate degradation is rare while the application of phosphate oxygen isotopes is non-existent, and there are not any previous attempts made to understand the oxygen isotopic fractionation during partial degradation of any organophosphorus compounds. This research investigated the bacterial phytate degradation kinetics in *Escherichia coli* and *Bacillus subtilis* as well as characterized the kinetics and pathways of enzymatic phytate degradation by a purified wheat phytase using a combination of novel analytical tools including NMR, HPLC, and phosphate oxygen isotope ratios ($\delta^{18}O_p$). The expression of phytate degradation activity by *E. coli* is potentially due to extracellular phytase activity, while the absence of activity in *B. subtilis* may be due to difference in position, synthesis, and regulation of phytase activity. Enzymatic phytate degradation results show that the inositol phosphate degradation undertakes two pathways, via D-I(1,2,3,5,6)P_5, D-I(1,2,5,6)P_4, D-I(1,2,6)P_3, and via D-I(1,2,4,5,6)P_5, D-I(1,2,5,6)P_4, D-I(1,5,6)P_3. Isotope results show that the cleavage of the P–O bond during inositol phosphate degradation is accompanied by the introduction of one oxygen atom solely from water to the released inorganic P. Interestingly, all phosphate moieties in inositol phosphate have the same $\delta^{18}O_p$ values, relieving the need to fully dephosphorylate inositol phosphate before measuring its isotopic composition of released phosphate. This means that tracking the original isotopic composition of inositol phosphate (with intact six phosphate moieties) can be done from its partially dephosphorylated products and this opens up the possibility of identifying original sources of partially dephosphorylated products that are still not fully degraded after they entered in soils many decades ago. Overall, these results advance fundamental understanding of biogeochemical cycling of inositol phosphate and could be used for dual purpose of identifying fate and tracking source of inositol phosphate in the environment.

Chapter 1

INTRODUCTION AND LITERATURE REVIEW

1.1 Introduction

Phosphorus (P) is a key nutrient essential for all living organisms. It serves in the phosphate-ester backbone of DNA and RNA as a redox-insensitive element providing stability to the fundamental molecule of life and plays a functional role in the transmission of chemical energy through the ATP molecule. Inorganic orthophosphate (PO_4^{3-} referred to as Pi hereafter), the most prevalent form of P in the lithosphere and biosphere, is a compound in which the P atom is surrounded tetrahedrally by four oxygen atoms (in 5 oxidation state and 4 coordination number). A variety of condensed phosphates including pyrophosphate and polyphosphate originate from sharing of oxygens in PO_4^{3-} ions. The next most common form of P, organophosphorus compounds (referred to as P_o hereafter), is a group of substituted phosphate esters in which P and C are linked through O as a P−O−C bond. In soil, P_o is found mainly in humus and other organic material, while P_i is derived from the mineralization process. When P_i concentrations are too low to meet the P requirements of living organisms, P_o can act as an important alternative source of P (Benitez-Nelson, 2000; Clark et al., 1999). On the other hand, high P_i concentrations could contribute to the algal growth in aquatic systems and result in eutrophication and other water quality issues.

Inositol phosphate（IP_x where x=1, 2,…6) is a common group of P_o compounds found in eukaryotic organisms, especially in plants (e.g., Turner et al., 2002; Turner et al., 2007). Despite the common occurrence of inositol phosphates in the natural environment, their role in global phosphorus cycling remains poorly understood due to analytical difficulties particularly in detecting their presence in the environment (Turner et al., 2002). Depending on the number of substituted phosphate groups in an inositol, prefixes such as mono, bis, tris, tetrakis, pentakis and hexakis (for 1, 2…6 phosphate groups, respectively) are used to distinguish them in the IUPAC nomenclature (IUPAC, 1971). Within a fixed number of phosphate groups attached in an inositol, a number of stereoisomers may be present. The *myo*-inositol hexakisphosphate is the most common isomer and is often referred to by different names such as phytic acid for a free acid

form, and phytate (Fig. 1) for a salt form (Shears and Turner, 2007). Through out this thesis, the term 'phytate' is used for inositol hexakis-phosphate (with six phosphate moieties, Fig. 1) unless otherwise mentioned and the symbol IP_x with appropriate subscript is used to indicate corresponding number of phosphate moieties (e.g., IP_5 for pentakis inositol phosphates).

Phytate is considered as an anti-nutrient because it can decrease the bioavailability of nutritionally important minerals such as calcium, magnesium, zinc, and iron by chelating strongly with them (Greiner et al., 1997). Phytate functions as the major storage form of P in seeds and is gradually enzymatically hydrolyzed to release orthophosphate during germination (Bassiri and Nahapetian, 1977). When present in soil, it is not directly available for plant uptake until it is hydrolyzed and Pi is released (Lung and Lim, 2006). It is also present in large amounts in aquatic sediments, where its degradation may contribute to eutrophication and thus pose a potential threat to water quality (Turner et al., 2002).

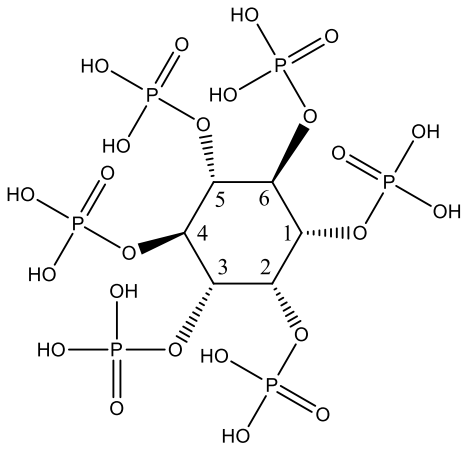

Fig.1. Chemical structure of myo-inositol hexakis-phosphate (phytate).

1.2 Degradation of Phytate

The phosphate ester linkages in phytate are quite stable, and abiotic degradation is almost impossible in alkaline environments (Turner et al., 2002). However, the degradation of phytate is rather fast in the presence of enzymes, within organisms (Mullaney and Ullah, 2003) such as such as roots, vegetative storage organs, pollen, and seeds (Williams, 1970; Rayboy, 2003), or blood of calves, birds, reptiles, and fishes (Haefner et al., 2005). It is unclear whether the phytase

enzyme exists free of cells in the natural environment. In general, the degradation can be divided into two classes: a) enzymatic degradation (cell-free enzymes), b) degradation by intact cells.

1.2.1 Enzymatic degradation of phytate

Phytases (*myo*-inositol hexakisphosphate phosphohydrolases) are defined as the group of phosphatase enzymes that catalyze the hydrolysis of phytate in a stepwise manner and release P_i (e.g., Greiner et al., 1997; Konietzny and Greiner, 2002). There are four different classes of phosphatases that are known to have phytase activity: histidine acid phosphatase (HAP), β-propeller phytase (BPP), cysteine phosphatase (CP) and purple acid phosphatase (PAP) (Mullaney and Ullah, 2007). The different catalytic mechanisms and some other features of different classes of phosphatase allow them to utilize phytate as a substrate under various conditions (Mullaney and Ullah, 2007). Microbial phytase initially hydrolyses the phosphoester bond at the 3' position, and is classified as 3-phytase (EC 3.1.3.8) while plant phytase attacks 6' phosphate first, and is named 6-phytase (EC 3.1.3.26). In general, phytase degradation of $IP_{2–3}$ is considerably slower than that of $IP_{4–6}$ and IP_1 degradation cannot be achieved by phytase (Kemme et al., 1999). Therefore phosphomonoesterase enzymes such as acid or alkaline phosphatase are used for IP_1 degradation. However, phosphomonoesterases can dephosphorylate IP_1 to IP_5 esters except IP_6 (Meek and Nicoletti, 1986; Shan et al., 1993).

Phytase are widespread in natural environments, including plants, animal tissues, and microorganisms. However, the phosphate in the phytate is not utilized by non-ruminant animals due to the lack of intestinal phytase. Phytate-degrading enzymes have been studied intensively in recent years because of their potential role in enhancing phytate utilization and P nutrition in animal feed and human food (Sandberg et al. 1996; Yi and Kornegay 1996; Greiner, 2007). Among different phytate-degrading enzymes, acidic phytate-degrading enzymes (with optimum pH around 5) and alkaline phytate-degrading enzymes (with optimum pH around 8) have been studied in detail (e.g., Konietzny and Greiner, 2002).

Pure phytases have been widely used to study phytate degradation (e.g., Greiner et al., 2000; Keruvuo et al., 2000; Nakano et al., 2000; Chen and Li, 2003; Greiner, 2004). Phytase extracted from different organisms or plants have different specificity as well as extent phytate degradation. For example, *Bacillus* phytase degrades only about half of the total phosphate

groups (Kerovuo et al., 2000). This means that *B. subtilis* can, at most, release three moles of P_i from one mole of IP_6, with *myo*-inositol trisphosphate as the end product. Furthermore, there are two alternative degradation pathways of IP_6 degradation by *Bacillus* phytase (Fig. 2). Phosphate in the 6' or 3' position in IP_6 is degraded first with different end products. Research on degradation pathway in *B. subtilis* has identified two independent routes: i) the first route that proceeds via *D*-I(1,2,3,4,5)P_5 to D-I(1,2,3,5)P_4 and finally to D-I(1,3,5)P_3, and ii) the second route that follows D-I(1,2,4,5,6)P_5 to I(2,4,5,6)P_4 and to I(2,4,6)P_3 as the end product. The phytate degradation pathway by phytase from *Escherichia coli* is different from that of *Bacillus* phytase (Greiner et al., 2000). As shown in Fig. 2, the *E. coli* phytase can degrade *myo*-inositol hexakisphosphate in a stepwise manner via D-I(1,2,3,4,5)P_5, D-I(2,3,4,5)P_4, D-I(2,4,5)P_3, I(2,5)P_2 and finally to I(2)P. As for enzymes from plants, degradation pathways of Na-phytate by wheat phytase (purified from wheat bran) have also been investigated (e.g., Nakano et al., 2000). Two wheat phytases (PHY1 and PHY2) follow the same major degradation pathway (Fig. 2), but could follow another minor route as well.

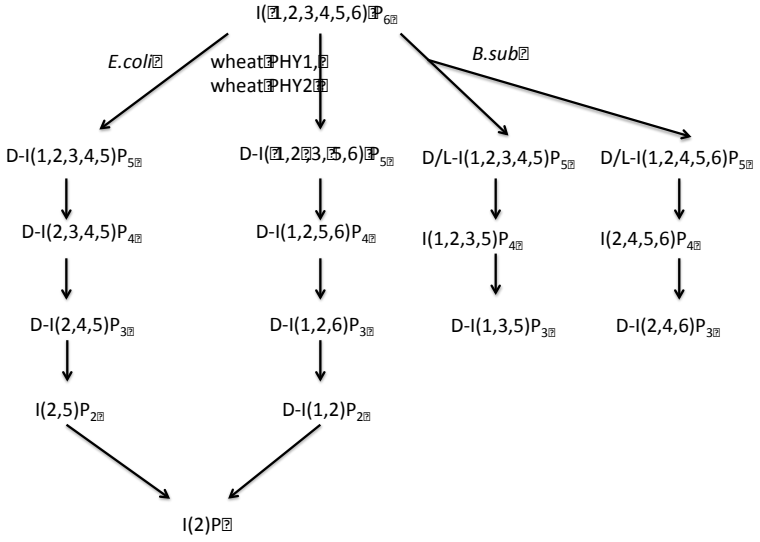

Fig.2. Phytate degradation pathways by different enzymes extracted from wheat and microorganisms (redrawn from Keruvuo et al., 2000; Greiner et al., 2000; Nakano et al., 2000).

1.2.2 Microbial degradation of phytate

While cell-free enzymatic studies have been widely used to understand phytase activity and degradation kinetics, intact cells from pure culture are not commonly used to degrade phytate. *Aspergillus* is the most common fungus species used primarily in food science to identify the degradation of phytate. *E. coli* and *Aspergillus ficuum* strains have been shown to rapidly degrade potassium phytate during fermentation in liquid media (Fredrikson et al., 2002). Similarly, lactic acid bacteria strains are also shown to degrade IP_6 during growth in flour (Reale et al., 2004). These studies are often performed in media with phytate as the sole P source so that microorganisms have to degrade phytate to obtain phosphate to support their growth. However, synthesis of phytase and expression of phytase activity varies among microorganisms and cannot be generalized. For example, the synthesis of phytase by *Klebsiella terrigena* often occurs during carbon starvation and is expressed in the later phases of growth (Greiner et al., 1997). For *E. coli*, the presence of phytate does not necessarily stimulate the production of phytase, yet it is found to be activated by phosphate limitation or anaerobiosis (Greiner et al., 1997). Phytase activity has been found to increase remarkably during the late stationary phase of cell growth (Greiner et al., 1993, 1997). Microorganisms with phytate degrading activity produce both intracellular and extracellular phytate-degrading enzymes (Hill and Richardson, 2007). For example, phytase synthesized by *E. coli* has been reported to be limited in the periplasmatic space (without any detached enzyme from cells; Greiner et al., 1993), but extracellular phytate degrading activity is detected in filamentous fungi (Konietzny and Greiner, 2002).

1.2.3 Abiotic degradation of phytate

The phosphate ester bonds in phytic acid are very stable, especially under basic conditions (Turner et al., 2002). Limited studies have been done so far to understand phytic acid stabilities in different pH conditions. The chemical/abiotic hydrolysis is slow and incomplete, with maximum hydrolysis occurring at pH 4.5 and minimum at pH 0–1 (Anderson, 1980). For example, the extent of degradation in the presence of concentrated HCl or HNO_3 at 100 °C was <<100% (Turner et al., 2002). These findings limited any additional studies on abiotic degradation of phytate.

Most recently, Sandy et al. (2013) found almost complete degradation of phytic acid

under intense (1200 W) ultraviolet radiation (UVR) photo-oxidation. The P_i release rate was high (2.31 μmoles/h) with more than 90% of phytic acid degraded within 72 h of the UVR treatment. In their study, the higher rate of P_i release from phytic acid than that from phosphonate was attributed to the relatively weaker P–O–C bond in phytic acid than the direct P–C bond in the phosphonate. While solar UVR is present in natural environments, albeit in extremely low intensity, phytate degradation by UVR could be a major abiotic pathway of phytate degradation in the natural environment, especially in regions with high solar incidences.

1.3 Oxygen Isotope Ratios of Phosphate as a Tracer to Understand P Cycling

Stable isotopes have long been used in biochemistry to understand reaction mechanisms due to the ease of labeling and characteristic effects of the labeled product during degradation reactions. Stable isotopes such as oxygen, nitrogen, sulfur, and carbon have been used to track elements during transfers between pools and to understand the respective roles of abiotic and biotic processes during transfer of labeled/non-labeled atoms (Jaisi and Blake, 2014). With ^{31}P being the only P stable isotope, tracing P cycling in the environment by using stable isotopes could not be performed like other nutritional elements such as C, N, and S that have multiple stable isotopes. Since P primarily occurs in most Earth environments as orthophosphate (P_i), the oxygen isotope ratios of the oxygen in phosphate can be used as a potential tracer for P cycling in the environment (Jaisi and Blake, 2014). By measuring the oxygen isotope ratios of released P_i and fractionation of oxygen incorporated in the released P_i, pathways of P_o degradation and P_i regeneration can be investigated (Blake et al., 1998). The isotopic composition of O in phosphate, which is expressed as $\delta^{18}O_p$, as:

$$\delta^{18}O_p = \left({R_{sample}}/{R_{standard}} - 1 \right) \times 1000$$

where R denotes the $^{18}O/^{16}O$ ratio, and R_{sample} and $R_{standard}$ refer to the ratio measured in the sample and the standard, respectively. The isotopic abundance is measured against a reference standard and is reported in delta notation in permil (‰) relative to the Vienna standard mean ocean water (VSMOW) standard.

1.3.1 Theoretical basis of isotope effects

The isotope effect relies on the principle that the zero point energy of a bond in any compound depends on the strength of the bond and the mass of the atoms involved in the bond. Therefore, depending on whether an atom in the compound is substituted with a lighter or heavier isotope, there will be corresponding isotope effects on reaction rates and reaction intermediates (Fig. 3). This means heavy-isotope substitution at the position of bond cleavage slows down the reaction because of a larger activation barrier for the heavy-isotope-substituted molecule (Lassila et al., 2011). Primary isotope effects result from isotopic substitutions at positions of bond cleavage or formation. Secondary isotope effects arise from changes in geometry or presence of heavy atoms in other sites in the structure. Because the sensitivity of isotope effects varies both with bond length and geometry, values of isotope effects are challenging to interpret, particularly in reactions performed in complex environments (Lassila et al., 2011).

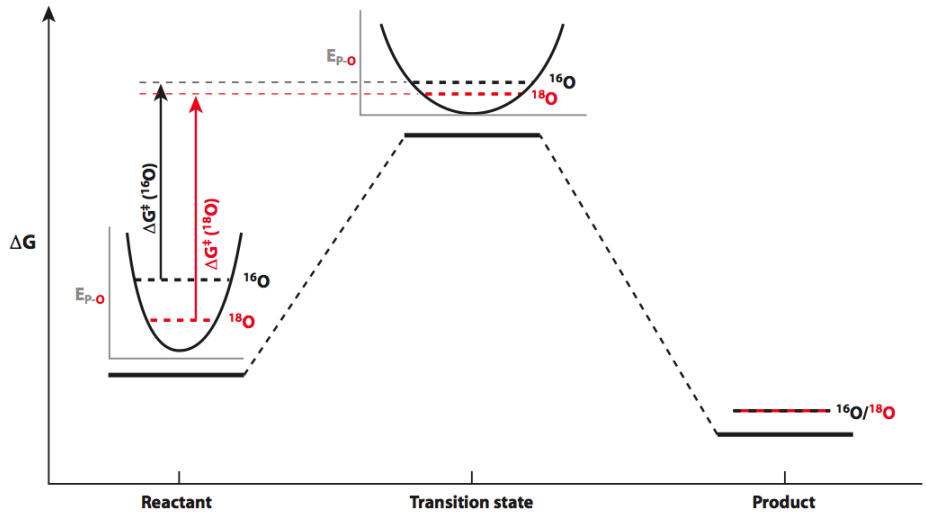

Fig.3. Difference in the free energy of ground and activated (transition) state of ^{18}O and ^{16}O during P-O bond cleavage imparts isotope effect (Lassila et al., 2011).

1.3.2 Oxygen isotope effects of organic phosphorus hydrolysis

Organic phosphorus degradation is catalyzed by the numerous phosphoenzymes in the environment. Major phosphoenzymes that are active in terrestrial and marine ecosystems include 5'-nucleotidase, peptidase, alkaline and acid phosphatase, aminopeptidase, phosphodiesterase,

and chitinase (Jaisi et al., 2014). Because biogeochemical cycling of P is dominated by enzyme-catalyzed biological reactions, isotope effects of specific phosphoenzymes could potentially be used to identify specific metabolic or enzymatic pathways (Liang and Blake, 2006a). However, the application of oxygen isotope ratios in P_o is not as straightforward as that for Pi since the organic phosphorus compounds normally contain extra oxygen atoms than that of phosphate moieties and measurement of isotopes requires separation of phosphate moieties from Po (Jaisi et al., 2014).

Among different enzymes, alkaline phosphatase (APase), which can hydrolyze a variety of organic phosphomonoester compounds and condensed inorganic phosphates, is the most common and most widely studied enzyme (Jaisi et al., 2014). Alkaline phosphatase degradation of phosphomonoesters results in the incorporation of one oxygen atom from the water in to the released phosphate (Liang and Blake, 2006a). While this is true for all monoesters, the kinetic fractionation factor during phosphomonoester degradation varies with the enzyme type and composition of the phosphomonoester (Liang and Blake, 2006a). The nature of bond breakage including the relative dominance of bond formation and bond breakage during phosphomonoester hydrolysis, determines the extent of the kinetic isotope effect (Lassila et al., 2011). The extent of water O incorporation is obtained from the slope of $\delta^{18}O_p$ values of released P_i vs the $\delta^{18}O_w$ values of ^{18}O labeled waters used in the hydrolysis experiments. For example, a slope of 0.25 during hydrolysis of adenosine 5'-monophosphate by 5'-nucleotidase (Fig. 4) suggests that the P_i released inherits three oxygen atoms from the PO_4 moiety group of original P_o and one oxygen atom derived from ambient water.

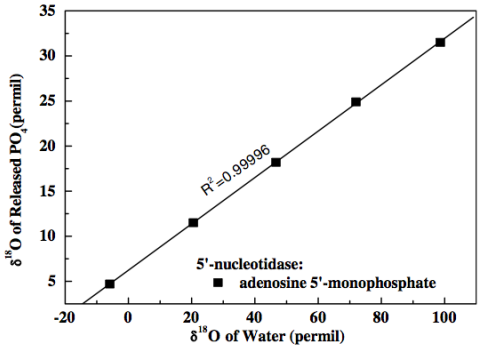

Fig. 4. Changes in $\delta^{18}O_p$ *values of released Pi as a result of oxygen atom incorporation from different* ^{18}O *labeled waters in adenosine 5'-monophosphate degradation catalyzed by cell-free 5'-nucleotidase (Liang and Blake, 2006a).*

Phosphodiester degradation is a two-step reaction. For example, for nucleic acid degradation, it involves the first-step cleavage of the polynucleotide backbone by endonucleases and then by exonucleases to free a nucleotide unit, the second-step cleavage of monoester linkages in the nucleotide is by monoesterase. A generalized degradation model cannot be applied for diesters because the reaction mechanism depends on the compound structure, compound elemental composition, and type of enzyme (Liang and Blake, 2009). For example, DNA and RNA are the two most common diesters but show different oxygen isotope effects during their hydrolysis because of their structural differences. The presence of an additional –OH group in the RNA structure compared to DNA allows the formation of cyclic 2',3'-phosphodiester intermediate during its breakdown and this intermediate allows extensive oxygen isotope exchange with water (Fig. 5). The slope of $\delta^{18}O_p$ of the released Pi and the $\delta^{18}O_w$ of water in DNA hydrolysis is ~0.45 (close to 0.5), which suggests two out of four oxygen atoms in the released phosphate are derived from the water and two oxygen atoms are inherited from DNA. On the other hand, the slope of $\delta^{18}O_P$ in the released phosphate and the $\delta^{18}O_w$ of water in RNA is 0.66, which is more than 0.5, indicating that more than two oxygen atoms in the released Pi are being incorporated from water. This is due to the isotope exchange between water and the 2',3'-phosphodiester intermediate. These results led Liang and Blake (2009) to develop the structure-based-reaction model for the oxygen isotope effects during phosphodiester hydrolysis.

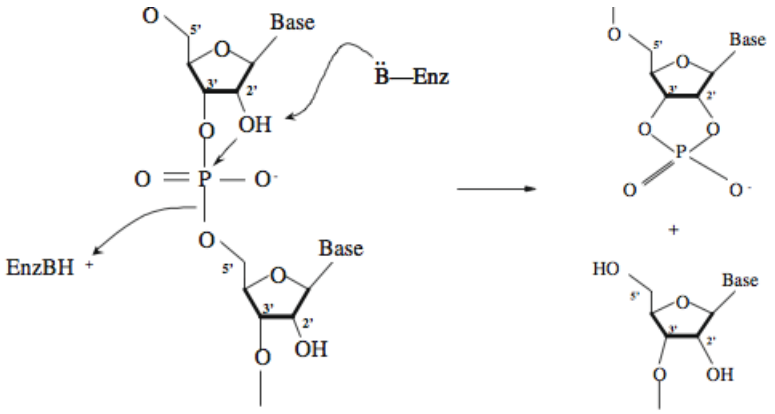

Fig.5. Formation of cyclic 2', 3'P-diesters during RNase catalyzed RNA degradation (Liang and Blake, 2009).

Isotope effects during abiotic degradation of P_o compounds depend on the method of degradation (Liang and Blake, 2006b, Sandy et al., 2013). For example, among dry combustion,

acid hydrolysis, and UVR methods studied so far, the dry combustion method promotes extensive oxygen isotope exchange between phosphate and atmospheric O_2 and thus erases the original $\delta^{18}O_{Po}$ values. Both acid and enzyme-catalyzed hydrolysis of P_o incorporate oxygen atoms from water into extracted Pi and thus $\delta^{18}O_P$ values of Pi extracted using these two methods only partially retain the original $\delta^{18}O_{Po}$ value. However, there are several differences of enzymatic and non-enzymatic hydrolysis of organophosphorus compounds. Additional theoretical aspects of the expected differences are listed in Jaisi et al. (2014) and are out of the scope of this research.

Among reduced organophosphorus compounds, hydrolysis research is limited to phosphonate (oxidation state of +3), in which phosphorus is connected directly to the carbon atom by a covalent bond. Ultra violate radiation degradation of two synthetic phosphonates (glyphosate and phosphonoacetic acid) in ^{18}O labeled water experiments showed the slope of ~ 0.18 rather than the multiple of 0.25 (Fig. 6; Sandy et al., 2013). Based on this result, these authors claimed that the oxygen atoms both from ambient water and atmospheric oxygen are incorporated during the C−P bond cleavage. Such results may be limited to UV photo-oxidation because the formation of peroxy radicals from excited organic molecules and atmospheric oxygen under the influence of UV photons (Braun et al., 1986) may promote incorporation of atmospheric oxygen to the released Pi.

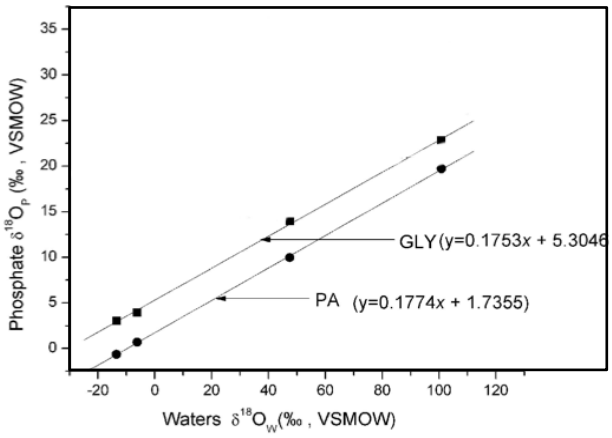

Fig 6. $\delta^{18}O_p$ values of released P_i and water used in the degradation of glyphosate (Gly) and phosphonoacetic acid (PA) hydrolysis by UVR photo-oxidation (Sandy et al., 2013).

1.4 Analytical Methods to Study Phytate Degradation

High-performance liquid chromatography (HPLC), nuclear magnetic resonance spectroscopy (NMR), and stable isotopes (C and P) are the major analytical methods to study mechanisms and pathways of phytate degradation.

1.4.1 High-performance liquid chromatography (HPLC)

Since the sequential phytate degradation produces multiple IP_x, identification and quantification of each degradation product is crucial in elucidating the degradation kinetics and identifying the degradation pathways. High performance liquid chromatography is the most powerful tool among all chromatographic techniques (Lindsay, 1992), and represents the most frequently used analytical technique in almost all chemical applications (Chester, 2013) compared to traditional electrophoretic and ultracentrifugal techniques. The automation of HPLC sampling, fraction collection, data generation, data reduction, and reporting functions are more versatile and have greatly improved quantification and output (Thayer et al., 1996). Although the separation of inositol phosphates by gas chromatography (GC) could resolve the identity of intermediate products much better, the need to volatilize compounds and transfer into capillary column precludes routine use of this method (Cooper et al., 2007). HPLC is considered to be a relatively sensitive and selective approach that can separate inositol phosphates effectively and efficiently (Turner et al., 2002) and has been widely used in detecting IP_x and elucidating the phytate degradation pathways (van der Kaay and van Haastert, 1995; Greiner and Larsson Alminger, 2001; Casals et al., 2002; Harland et al., 2004; Greiner, 2004).

1.4.2 Nuclear magnetic resonance (NMR) spectroscopy

NMR is a versatile method that can provide complete structural information of phytate and its degradation products. Inositol phosphates contains three NMR-active nuclei (^{1}H, ^{31}P, and ^{13}C); therefore detailed information about the structure of the parent inositol moiety and the number and positions of phosphorylation on the ring can be obtained by combining information from these three nuclei (Murthy, 2007). An additional benefit of using NMR is that it is capable of distinguishing between similar compounds in complex matrices (Nanny and Minear, 1994), as well as analyzing individual components without prior separation of samples (Murthy, 2007).

This advantage makes NMR an attractive technique in speciation of inositol phosphate, its partially dephosphorylated products and other organic P compounds. Compared with HPLC, NMR does not necessitate standards that may cause background matrix effects while providing simultaneous determination of P groups in the same run (Kemme et al., 1999; Turner et al., 2003). However, application of standards or model compounds greatly improves resolving peak identity of individual inositols.

Because ^{31}P is the only naturally abundant P stable isotope, all P species in a phytate and partially dephosphorylated products can be detected by NMR spectroscopy (Kemme et al., 1999; Cade-Menun, 2005). Identification of compounds using ^{31}P NMR is based on their chemical shifts relative to an external H_3PO_4 standard (Turner et al., 2003) and quantification of different P forms in a sample is based on the peak area, which is proportional to the number of particular type of P nuclei (Cade-Menun, 2005). The sensitivity of ^{31}P NMR was reported to be 25±0.05 mM (Lipok et al, 2009). While uncoupled ^{31}P NMR can be used to quantify different P forms and has been most widely used, ^{1}H coupled NMR could provide another parameter to better resolve the identification of different P forms.

Phytate and its degradation products generate several NMR peaks. To identify these peaks, ^{31}P resonance peaks are assigned to individual IP_x compounds on the basis of simultaneously appearing and disappearing peaks during phytate degradation (Kemme et al., 1999). ^{1}H-decoupled NMR spectra can provide additional information on the detailed degradation kinetics as well as enable quantitative determination of residual inositol phosphates. Further confirmation of peak identity can be established through comparison of $J_{1H,31P}$ coupling constants. For three bond coupling as is the case for phytate and its degradation products, the coupling constant ($^{3}J_{1H,31P}$) has been reported to be in the range of 5-10 Hz (Hoffman, 2013). While coupling constants are not often used, this additional parameter is useful to resolve IP_x composition especially when different products have similar chemical shifts.

1.4.3 Oxygen stable isotope ratios in phyate and degraded phosphate

Oxygen isotopes could be a promising tracer for phytate degradation during bacterial and enzymatic degradations. To date, no isotopic study on phytate degradation has been performed. Because phytate has a limited number of oxygen moieties (4−6 as OH, depending on pH) besides

the oxygen in phosphates (which have 24 oxygen atoms), direct measurement of $\delta^{18}O_p$ values comes overwhelmingly from phosphates in phytate. Measurement of $\delta^{18}O_p$ values at different time points during phytate degradation in the presence of labeled water enables understanding of the mechanism under which oxygen atoms are incorporated in the released phosphate. It will also test whether the isotope effect varies with different phosphate moieties in the inositol ring. Combination of HPLC, NMR, and stable isotopes can collectively help constrain the degradation pathways, and provide a cohort of new tools that can be used to understand the degradation and detect degradation products from phytate in natural environments.

Chapter 2

RESEARCH OBJECTIVES, MATERIALS AND METHODS

2.1 Research Objectives

The major objectives of this thesis research are as follows:

i) To understand the phytate degradation kinetics catalyzed by cell free enzymes and intact bacterial cells (*Bacillus subtilis* and *Escherichia coli*)

ii) To identify intermediate degradation products and generate phytate degradation pathways using nuclear magnetic resonance spectroscopy (NMR) and phosphate oxygen stable isotope ratios ($\delta^{18}O_p$).

2.2 Materials and Methods

To understand phytate degradation, phytate, phytase, and microorganisms were purchased. Additionally model phytate compounds with partially dephosporylated inositol phosphates as well as ^{18}O labeled air and waters were purchased to resolve NMR peaks and identify isotope effects, respectively during phytate degradation. Phytic acid dipotassium salt (inositol hexakisphosphate), D-*myo*-inositol 1,2,4,5,6-pentakis-phosphate, *myo*-Inositol 1,3,4,6-tetrakis-phosphate ammonium salt, L-myo-inositol 1,4,5-tris-phosphate potassium salt and wheat phytase (E.C. 3.1.3.26) were purchased from Sigma-Aldrich. Two bacterial strains, *Bacillus subtilis* (ATCC 23857) and *Escherichia coli* (ATCC 33965), were purchased from American Type Culture Collection (ATCC). 98% ^{18}O labeled air and 10% labeled water were purchased from Icon Isotopes.

2.2.1 Enzyme purification

Pilot experiments showed that the commercial wheat phytase (Sigma) was a crude extract containing high amounts of inorganic P and potentially other enzymes. Therefore the crude wheat phytase was purified in the Protein Production Core Facility at the Delaware Biotechnology Institute (DBI). Purification followed the protocol of Brejnholt et al. (2011). In

brief, for every 5 g crude phytase extract, 20 mL buffer A (0.1 M sodium acetate pH 4.3 with 1 mM calcium chloride) was added to dissolve the crude extract. The solution was then centrifuged at 6,000 × g for 30 min at 4 ºC. The supernatant was collected and saturated ammonium sulfate solution was added slowly to 30% saturation. The solution was then stirred on ice for 20 min and clarified by centrifugation at 13,000 × g at 4 ºC for 15 min. The supernatant was collected again and ammonium sulfate precipitation was repeated to 60% saturation. The pellet was collected after centrifugation at 13,000 × g for 15 min and resuspended in 8 mL buffer A. The phytase solution was then desalted using a PD-10 column (GE Healthcare). The enzyme was further purified by a HiTrap SP cation exchange column (GE Healthcare) using buffer A and a linear gradient of buffer A + 0.5 M NaCl. Fractions were collected and sodium dodecyl sulfate (SDS) gel electrophoresis was performed to confirm a protein band with approximate molecular weight 60 kDa. Those fractions suspected to contain enzyme activity were tested using 1 mM phytate solution. The fractions displaying enzyme activity were pooled together and concentrated using an Amicon Ultra 15 centrifugal device (Millipore) and included on the purification steps (above). Non-specific phosphatase activity was also determined by testing the purified enzyme with p-Nitrophenyl phosphate (pNPP) substrate (Maenz and Classen, 1998).

2.2.2 Bacterial phytate degradation experiments

B. subtilis and *E. coli* stocks obtained from ATCC were propagated in nutrient broth and Luria-Bertani (LB) medium, respectively, and the grown cells were used to prepare frozen stocks in 15% glycerol and stored at –80 °C. In later experiments, the frozen stocks were revived and grown in their respective media for 24 hrs, to late-log phase at their optimal growth temperatures, followed by centrifugation at 4000 rpm and re-suspension in minimal media that consisted of 10 g/L glucose, 2 g/L $CaCl_2$, 5 g/L NH_4NO_3, 0.5 g/L KCl, 0.01 g/L $FeSO_4$, 0.01 g/L $MnSO_4$, and 25mM Tris-HCl, pH 7.5. The bacterial phytate degradation experiments were performed with cells dispersed in this media using 1.0 mM potassium phytate as the sole P source. All handling and sampling in these experiments was conducted under sterile conditions in a biosafety cabinet or on sterile benchtop.

At selected time points, aliquots of cell culture were withdrawn to quantify released P_i as the result of phytate degradation using the phosphomolybdate blue method (Murphy and Riley,

1962). Total P in the solution as well as inside cells was quantified using inductively coupled plasma optical emission spectrometry (ICP-OES). The number of cells in the culture over time was monitored using optical density measurements as well as serial dilution and plate counts. Analysis of speciation of P in cell culture were performed based on total P in the solution, supernatant P without cells, Pi in the supernatants, and cell P in the pellets.

2.2.3 Enzymatic phytate degradation in ^{18}O labeled water and air

A typical enzymatic phytate degradation experiment included 0.4U purified phytase with 100 mL of 1 mM potassium phytate solution prepared in Na-acetate buffered at pH 5.5. The experimental set up was incubated at 55 °C. The control experiment was performed in the same buffer but without adding any phytase. Samples were withdrawn at 1, 2.5, 4.2, 24, and 48 hrs (based on degradation kinetics from the preliminary experiment) and the degradation reaction in each aliquot was stopped by adding 1M HCl at a 1:1 ratio (Adeola et al., 2004). Each sample was split for P_i quantification, NMR analysis, HPLC analysis, and oxygen isotope ratios measurements. The amount of released P_i was quantified by using the phosphomolybdate blue method (Murphy and Reily,1962) as above.

^{18}O labeled water reactions were carried out in in phytate solution described above prepared using seven different waters with a wide range of $\delta^{18}O_w$ (-7.0−74.0‰) in order to detect the incorporation of oxygen from ambient water into released phosphate during the degradation of inositol phosphate. In selected labeled water phytate solutions, additional phytase enzyme was added after 24 hrs of incubation to test additional phytate degradation. Reactions were carried out under optimal conditions (e.g., pH, temperature, and buffer) specified by the manufacturer (Sigma Aldrich). $\delta^{18}O$ values of water in the reactions were measured at the start and the end of each experiment.

To investigate the role of atmospheric oxygen incorporation into released phosphate during enzymatic degradation of phytate, ^{18}O labeled air experiments were set up by diluting the highly enriched (98 atom %) oxygen air into final $\delta^{18}O_{O2}$ values of 43, 95, and 160 ‰. Labeled air was serially diluted into serum bottles inside a glove box to avoid any contamination from ambient oxygen in the air. To ensure complete diffusion of labeled air with dissolved air in the phytate solution, enzyme addition and incubation was delayed for about 6 hrs after labeled

oxygen was injected into the headspace. All experiments were carried out in 120 mL serum bottles with the phytate solution described above under sterile conditions at 55 °C in a temperature-controlled (±0.5 ^{o}C) incubator. Other experimental conditions, sampling, and sample analyses were the same as labeled water experiments.

2.3 Analytical Methods

2.3.1 HPLC analysis

To test the consistency of inositol phosphate quantification by HPLC and NMR methods along with Pi quantitation by the colorimetric method, the same samples were used in both studies. Samples withdrawn at series of time points in the enzymatic phytate degradation experiment performed at 10 ‰ ^{18}O labeled water were chosen for comparison. Please note that the kinetics and extent of phytate degradation were found not to be impacted by the $\delta^{18}O_w$ value of labeled waters.

For HPLC analyses, aliquots of samples were freeze-dried and then dissolved in 0.54 mL of 0.5M NaOH and 0.06 mL D_2O. All HPLC measurements were performed at the Max Rubner-Institut, Karlsruhe, Germany. In brief, samples were appropriately diluted and chromatographed on an HPLC system using a Pharmacia HR5/5 (5 cm) column and a gradient of HCl (0.005 to 0.5 M; flow rate of 1mL/min). To achieve post-column derivatization, the eluents were mixed with 0.1M HCl that containing 5.18 mM $FeCl_3$ and 0.25 M NaCl via the twisted PTFE coil (length 8 m; i.d. 0.5mm) (HPLC-pump 2248, Pharmacia; flow rate: 0.8 mL/min). Peaks were identified by addition of inositol phosphate standards.

2.3.2 NMR analysis

Samples withdrawn at different time points from the enzymatic phytate degradation experiment performed in 10 ‰ ^{18}O labeled water were freeze-dried and then dissolved in 0.54 mL of 0.5 M NaOH and 0.06 mL D_2O (Cade-Menun and Liu, 2013). To distinguish the peak positions and to resolve the identity of the partially degraded phytate products, NMR peak positions of model compounds were measured. These included pure *myo*-inositol phosphates phytic acid dipotassium salt, D-*myo*-inositol 1,2,4,5,6-pentakis-phosphate, *myo*-Inositol 1,3,4,6-

tetrakis-phosphate ammonium salt and L-*myo*-Inositol 1,4,5-tris-phosphate potassium salts. These pure inositol compounds were first dissolved in 0.6mL 0.52 M NaOH prepared in D_2O to obtain final concentrations of 0.33-7.0 mg/mL. Proton-coupled （32 number of scans) and decoupled (16 number of scans) ^{31}P NMR measurements were performed at 9:1(H_2O: D_2O) ratio in AV 400 MHz Bruker NMR spectrometer operating at 161.97 MHz for ^{31}P at the University of Delaware. All measurements were carried out at room temperature (23 °C) and all peak shifts were calibrated to the external standard of 85% phosphoric acid. Identification of phytate degradation products using ^{31}P NMR was based on their chemical shifts, peak area and coupling constants.

2.3.3 Analysis of oxygen isotope ratios in ^{18}O labeled water and air experiments

The released P_i from ^{18}O labeled water and air experiments was processed for silver phosphate precipitation using methods described in Jaisi and Blake (2010). This involved a series of precipitation and dissolution steps to remove other media and reagent components. In brief, P_i was precipitated first as ammonium phosphomolybdate (APM), dissolved, and then precipitated as magnesium ammonium phosphate (MAP). The sample was further treated with cation resin to remove residual cations. Finally, the purified phosphate was precipitated as silver phosphate for the phosphate oxygen isotope measurement. The silver phosphate was then roasted at 107 °C for 12 hrs to remove any remaining and trapped water. Silver capsules that contain 200−300 μg of silver phosphate were prepared in triplicate for oxygen isotope analysis.

All phosphate O isotope measurements were carried out at the stable isotope facility at the University of Delaware. Silver phosphate was analyzed by online high-temperature thermal decomposition using a Thermo Chemolysis/Elemental Analyzer (TC/EA) coupled to a Delta V continuous flow isotope ratio monitoring mass spectrometer (IRMS; Thermo-Finnigan, Bremen, Germany) with precision of ±0.3 ‰. The $\delta^{18}O_p$ values of silver phosphate samples were calibrated against the conventional fluorination method using two internal laboratory silver phosphate standards arbitrarily designated as YR1a and YR32 with $\delta^{18}O_p$ values of −5.49 and 33.63 ‰, respectively (Venneman et al., 2002). Samples and standards were run at least in triplicate. All oxygen isotope data are reported as $\delta^{18}O$ ‰ relative to Vienna standard mean ocean water (VSMOW) as a reference standard.

Linear regressions of $\delta^{18}O_p$ values of released P_i vs $\delta^{18}O_w$ values of water or air used in the experiments were performed to identify the slope and the fractionation for water (between ambient and incorporated in Pi) $\delta^{18}O_w$ values. Based on these results, isotope effects of specific degradation pathway or specific reaction mechanisms were identified.

Chapter 3

PHYTATE DEGRADATION KINETICS AND PATHWAYS

3.1 Bacterial Phytate Degradation

Bacillus subtilis and *Escherichia coli* cells were first grown in nutrient-rich medium, washed and resuspended in buffer before transferring them into minimal medium/phytase screening medium (Kerovuo et al., 1998) that contains 1 mM phytate as the sole P source. Dissolved phytate reacted with Ca^{2+} and Fe^{2+} ions present in the growth media and formed Ca-phytate or Fe phytate precipitate, producing a cloudy suspension. This phenomenon could be explained by the higher ability of phytate to chelate metal ions and formation of metal-phytate complexes as precipitates. For example, formation of Ca-phytate complexes have been found to dissolve calcite (Celi et al., 2000) and similarly Fe and Al-oxides (Shang et al., 1990; Ognalagna et al., 1994; Johnson et al., 2012). Several pilot experiments in this research aimed at investigating the microbial degradation of phytate precipitate (as Ca-phytate formed under the medium pH of 7.5, or Fe-phytate formed at other pH values), showed that phytate degradation was insignificant, suggesting that P in Ca or Fe-phytate is relatively unavailable for microorganisms. This result is consistent with literature that the formation of a metal-phytate complex affects physical, chemical, and biological processes controlling solubilization and bioavailability of phytate, and transforms otherwise labile phytate P into more recalcitrant P (Zhang et al., 1994). To avoid the formation of phytate precipitate, the calcium chloride concentration in the media was adjusted to that of M9 minimal media (Miller, 1972) from 20 mM to 0.1 mM. No phytate precipitate was observed in this modified medium and as expected, phytate degradation was observed (Fig. 7). As is shown in Fig. 7a, Pi concentration in the media with *E. coli* reached almost 4000 μM at 120 hrs of incubation (~400%, with theoretical possibility of 600%, as 6 moles of Pi are released from a mole of phytate). These results suggest the presence of extracellular phytase activity in *E. coli* strain. This result is consistent with the presence of two different phosphatases (*agp*-encoded acid phosphatase and *appA*-encoded phosphatase) in the periplasmic layer of *E. coli.* The *agp*-encoded phosphatase has specificity for hydrolyzing D-3 phosphate residue in phytate (Cottrill et al., 2002), while *appA*-encoded

phosphatase sequentially removes five out of six phosphate groups in phytate with phosphate at D-6 position dephosphorylated first (Greiner et al., 2000).

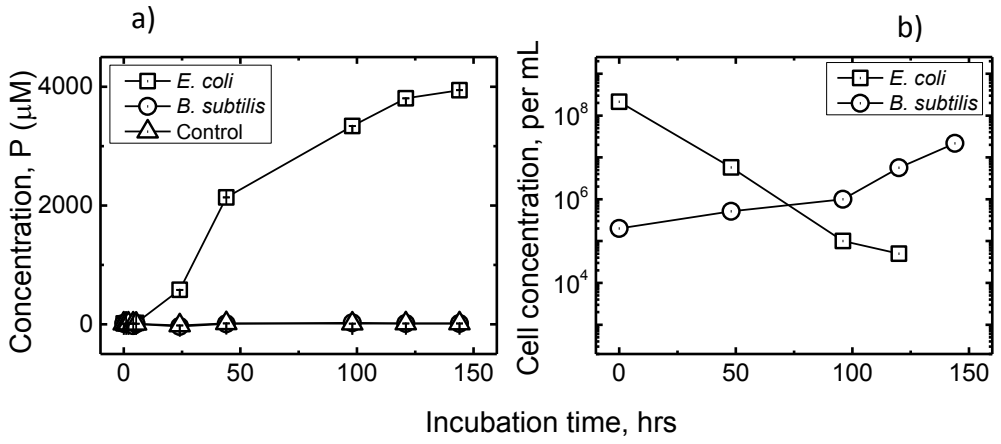

Fig. 7. a) Kinetics of phytate degradation by Escherichia coli and Bacillus subtilis in the minimal medium and, b) their growth shown as cell numbers over time.

There was no phytate degradation activity detected in the *Bacillus subtilis* culture (Fig 7a). To ensure that these results were reproducible, experiment was repeated, and changes in solution chemistry before and after the experiment were measured and P mass balance calculated. Cell growth measured over incubation times both by plate counts and by optical density (A600 nm), however, showed that the cell concentration increased over incubation time (Fig. 7b) while no significant amount of Pi was released due to phytate degradation. This could be attributed to expression of intracellular phytase activity of *B. subtilis* strain and the efficient use of P from degraded phytate for their own growth, i.e., without releasing P in the media. However, the changes in P in the cells were too low to reliably measure and account P uptake and transformation in the cells. Absence of phytase activity might also be due to incubation conditions being less than optimal for the expression of phytase activity by *B. subtilis* (see below).

Bacterial phytate-degrading enzyme syntheses are turned off in exponential phase and initiate as soon as the cells enter stationary phase in non-limiting media (Greiner, 2007). Nutrient or energy limitation, which could occur in the stationary phase, was suggested to induce the synthesis of phytase (Greiner et al., 1997). Formation and expression of phytate-degrading

enzyme in microorganisms is complex, yet non-uniform regulation among various conditions has complicated the generalization (Konietzny and Greiner, 2004). For example, it was reported that only carbon starvation along with the presence of phytate could provoke the synthesis of phytase by *Klebsiella terrigena* among other nutrient limitations tested (Greiner et al., 1997). The formation of a phytate-degrading enzyme in *E. coli* was found to be stimulated by phosphate starvation, while carbon, nitrogen, and sulfur limitation were impotent (Touati et al*.,* 1987). A likely explanation for why *B. subtilis* did not express phytase activity is that phytase formation depends on other nutrient, pH, and incubation conditions similarly to *K. terrigena* in which carbon limitation promotes phytase synthesis. However, a slight increase in *B. subtilis* growth (Fig. 7b) is the consequence of orthophosphate (derived from phytate) uptake into cells.

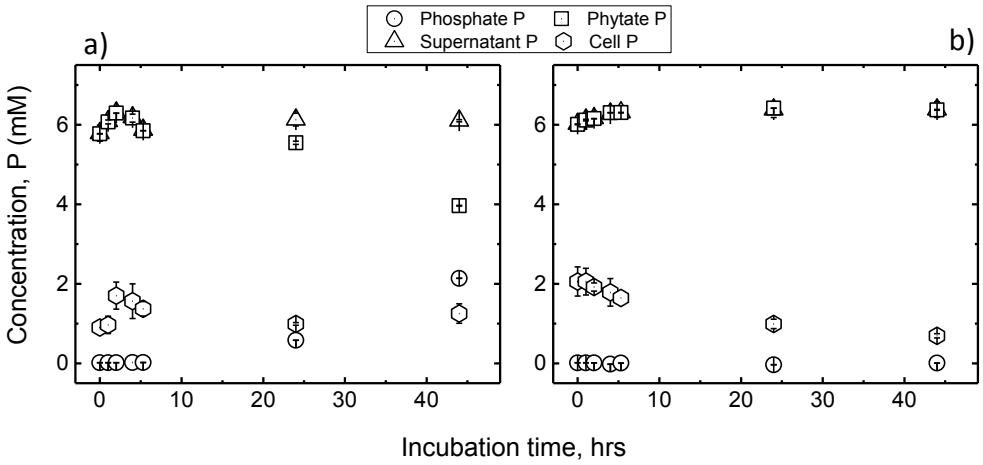

Fig. 8. Speciation of P in E. coli (a) and B. subtilis (b) culture into total P, cells P, supernatant Pi and phytate P. Phytate P was calculated by subtracting the Pi in the supernatant from the total P in the culture. P concentrations are expressed as μM.

Speciation of P during bacterial phytate degradation is presented in Fig 8. To be consistent, all P measurements were based on ICP-OES except Pi in the supernatant that was measured colorimetrically. As shown in the figure, concentrations of total P and supernatant P were similar, which can be explained by the relatively low amount of P stored inside cells. The low cell P is rather unexpected because cell components (nucleic acids, lipids, ATP) and cell storage (orthophosphate, polyphosphate, and pyrophosphate) together contribute a significant amount of P in cells. A potential reason for this could be lower sensitivity of ICP measuring cell

P. The increase of Pi corresponding to the decrease in inositol phosphate in the *E. coli* culture indicates that the Pi was generated by the degradation of inositol phosphate and released into the solution. There might be other organic P besides inositol phosphate present in the supernatant particularly in the later part of the experiments due to potential release of organic P from cell death and lysis. Because we did not see a spike in any P pool, contribution of such unknown organic P is expected to insignificant.

3.2 Enzymatic Phytate Degradation Kinetics

Degradation of phytate by purified phytase enzyme showed rapid release of Pi first followed by slow but continuous Pi release for up to 140 hrs (Fig. 9). For example, phytate degradation achieved ~450% yield (i.e., 4.5 moles of Pi released from one mole of phytate) after 24 hours of incubation. In the control experiments without phytase, the amount of released Pi was negligible, which suggested that the non-enzymatic hydrolysis of phytate under the experimental conditions and time is not likely to happen. As shown in Fig. 9, Pi yield reached ~ 500%, suggesting that the wheat phytase could at least remove five phosphates from the inositol ring.

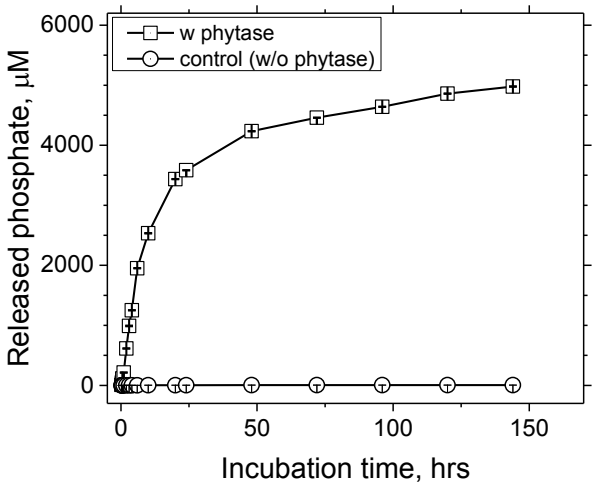

Fig. 9. Phytate degradation kinetics of purified phytase from wheat.

Previous research shows that purified phytases can degrade phytate only up to inositol monophosphate (containing one phosphate moiety in the inositol ring) and inositol 2-phosphate

was the final degradation product (Konietzny and Greiner, 2002). The inositol monophosphate can only be degraded under high phytase concentration with prolonged incubation or by the activity of other nonspecific phosphomonoesterase (Greiner, 2007). Because the degradation was limited to about 500% in this study, it indirectly verifies that the purified enzyme was free from unspecific phosphomonoesterase that could release phosphate from inositol monophosphate (IP_1).

3.3 Identification of Phytate Degradation Products

3.3.1 HPLC analysis of degradation products and phytate pathways

Partially dephosphorylated IP_x products generated at different time points phytate degradation are shown in Table 1. The inositol phosphate degradation follows a stepwise manner in which partially degraded products serve as intermediate substrates for further degradation. For example, I(1,2,3,4,5)P_5 concentration at 1 hr was very high and rapidly dropped to an insignificant quantity at 2.5 hrs, suggesting rapid degradation of IP_6 to IP_5 as well as a short half-life of IP_5 intermediates. Among four different IP_5 isomers detected, the I(1,2,4,5,6)P_5 isomer is produced in low quantity and the rate of degradation is slow compared to that of the (1,2,3,4,5)P_5 isomer. I(1,3,4,5,6)P_5 and I(1,2,3,4,6)P_5 isomers are present in trace amounts at all times suggesting these two isomers could have been produced in infinitesimally small quantity but were degraded completely after 48 hrs of reaction. Furthermore, I(1,2,5,6)P_4 was the most dominant IP_4 isomer and remained accumulated in the product until after 4.2 hrs. The identification of IP_2 and IP1 is limited due to the lack of a proper standard because these are new species not identified so far. Total P mass balance at different time points accounting Ps in partially dephosphorylated inositol phosphate was good. Overall, these results show formation of multiple isomers with different half-lives indicating more than one degradation pathway and potentially different isotope fractionation factors.

Depending on the position where the susceptible phosphoester bond is initially attacked, phytases are classified into two classes: i) 3-phytase (EC 3.1.3.8), which removes phosphate initially from the D-3 position of the *myo*-inositol ring, and ii) 6-phytase (EC 3.1.3.26), which preferentially initiates inositol phosphate degradation at the L-6 (D-4) position. The cereal phytases from wheat, spelt D21, rye, barley P1 and P2, and oat were identified as 6-phytases (Greiner and Alminger, 2001), which preferentially initiate the cleavage of phosphate at the L6

(D-4) position on the *myo*-inositol ring. Wheat phytase is a plant phytase expected to have the 6-phytase activity that initially removes phosphate on the 6' position. Even though most phytases studied so far fit into this classification, there are exceptions and thus this rule does not characterize all phytases.

Table 1. Time course change in dephosphorylated inositol products from the degradation of phytate by wheat phytase. IP_2 and IP_1 concentrations were too low to be detected by HPLC.

Time, hrs	*Phytate degradation products, μM*						
	I(1,2,3,4,5,6)P_6	*I(1,2,3,4,5)P_5*	*I(1,2,4,5,6)P_5*	*I(1,2,5,6)P_4*	*I(1,2,3,4)P_4 /I(1,3,4,6)P_4*	*I(1,2,6)P_3/ I(1,2,3)P_3*	*I(1,5,6)P_3*
1	572.5	704	99.8	238.1	64	0	42.5
2.5	26.2	74.9	27.4	549.4	127.6	3.4	178
4.2	32.9	28.5	34.7	355.2	65.6	55.8	343.8
24	26.8	9.2	16.7	53.8	9.3	101.5	41.5
48	14.7	3.3	9.5	7.2	0	77.3	23.3

Based on the HPLC results that account for different IP_5, IP_4, IP_3 and their isomers in the degradation products (Table 1), a potential pathway of inositol phosphate degradation by wheat phytase is generated (Fig. 10). As shown, there are two different pathways: i) the major degradation pathway is via D-I(1,2,3,5,6)P_5, D-I(1,2,5,6)P_4, D-I(1,2,6)P_3. This pathway is the same as published by Nakano et al. (2000) in which I(1,2,3,4,5,6)P_6 degrades in the order of D-I(1,2,3,5,6)P_5, D-I(1,2,5,6)P_4, D-I(1,2,6)P_3, D-I(1,2)P_2 and finally to I(2)P. ii) the minor pathway is via D-I(1,2,3,5,6)P_5, D-I(1,2,3,6)P_4, D-I(1,2,6)P_3. This pathway is comparable to that of wheat phytase F2 by Lim and Tate (1970). These authors used a pH of 7 to 7.5 for their studies, but perhaps F2 phytase also has some activity at pH 5.5 and follows: I(1,2,3,4,5,6)P_6, D-I(1,2,3,5,6)P_5, D-I(1,2,3,6)P_4, I(1,2,3)P_3, D-I(1,2,)P_2 to finally I(2)P. The minor pathway is new and has not been detected in wheat phytase before. However, the HPLC data show that the inositol phosphate degradation by wheat phytase is initiated at both the 6' phosphate and 3' phosphate positions, which resulted in the formation of both D-I(1,2,4,5,6)P_5 and D-I(1,2,3,5,6) P_5 isomers. This suggests the presence of another phytase with 3-phytase activity or that one of the wheat phytases has some 3-phytase activity and generates D-I(1,2,4,5,6)P_5 from phytate. This

IP_5 could be further degraded by one of the phytases or other phosphatases in the preparation to D-I(1,2,5,6)P_4 and D-I(1,5,6)P_3.

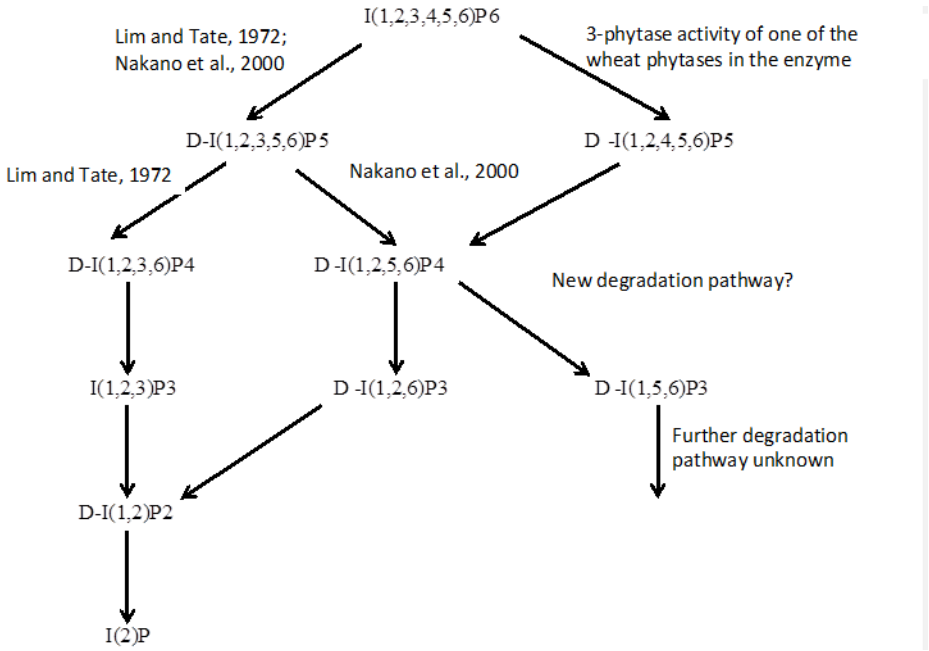

Fig 10. Phytate degradation pathways deduced from HPLC results. Please note that the additional degradation from D-I(1,5,6)P_3 is unknown as it does not fit any product from previous published results.

The final degradation product of the majority of inositol phosphate-degrading enzymes, regardless of their origin, is *myo*-inositol 2-phosphate (Greiner, 2007). Nonspecific phosphatase particularly from microorganisms can degrade the phosphate moiety in the 2' position (Kerovuo et al., 2000). Thus far, no phytase has been reported that can remove phosphate at the 2' position of the *myo*-inositol ring. Interestingly, our results show that D-I(1,5,6)P_3 is the most dominant degradation product that has a phosphate moiety in the 2' position degraded. This likely indicates the presence of unknown phytase or phosphatase with unknown activity in the wheat phytase. Further research is needed to identify and characterize this phytase enzyme.

3.3.2 ^{31}P and ^{1}H-^{31}P NMR results

^{31}P NMR spectra of partially dephosphorylated inositol phosphates generated during enzymatic phytate degradation at different time points are shown in Fig. 11. Because a single inositol phosphate generates several peaks and superimposed peaks from coexisting products

complicate peak identity, partially dephosphorylated phytate compounds were purchased and their peak positions were individually identified (Table 2). NMR spectra of these model inositol phosphates provided information on NMR shift and proton coupling information. Furthermore, the peak integration ratios of these pure inositol phosphates correspond to the symmetry of the phosphate moiety in *myo*-inositol structure. As shown in Fig. 1, *myo*- structure is symmetrical at the 2 and 5 positions, thus validating the results presented in Table 2. In this study, NMR peaks at different time points were analyzed by assigning the peaks (Fig. 11) based on their chemical shifts and peak area information gathered from model compounds as well as taking account on the simultaneously appearing and disappearing peaks during the degradation time course. For simplification, each degradation product (IP_x) was assumed to retain stereochemistry after phosphate hydrolysis and as a result all products are assumed to be *myo*- form. With that assumption, the ambiguity in HPLC data for D-I(1,2,6)P_3/ I(1,2,3)P_3 has been deduced to be D-I(1,2,3)P_3.

Table 2. ^{31}P NMR parameters for pure IP_x compounds.

Inositol Phosphates	*no. of Peaks*	*Peak area ratio*	*Shift (ppm)*	*$^3J_{1H,31P}$ (Hz)*
Phytic acid dipotassium salt	4	1:2:2:1	5.1:4.3:3.9:3.7	11.74
D-myo-inositol 1,2,4,5,6-pentakis-phosphate	4	1:1:2:1	4.6:4.2:3.9:3.5	8.8:11.7:8.8:7.9
myo-Inositol 1,3,4,6-tetrakis-phosphate ammonium salt	2	1:1	4.6:3.6	7.9:6.0
L-myo-Inositol 1,4,5-tris-phosphate potassium salt	3	1:1:1	4.88:4.77:3.19	8.8:5.9

The ^{31}P NMR spectra of phytate degradation products show compositional changes in type and amount of IP_x during phytate degradation, indicating a stepwise degradation process. Due to relatively lower sensitivity of ^{31}P NMR compared with HPLC, P species with concentration lower than its sensitivity limit (~250 μM) are difficult to identify without a good confidence, therefore are not presented. Please note the experimental solution was concentrated

by 5-18 times by freeze drying and subsequent dissolution on D_2O (see method). The ^{31}P NMR spectra (Fig. 11) shows the spectra of IP_6, IP_5, IP_4, IP_3 as well as orthophosphates as products generated within 1 hr of reaction. These partially dephosphorylated IP_X could compete as new substrates for phytase. It is interesting to note that the peaks for IP_6 and IP_5 almost disappeared

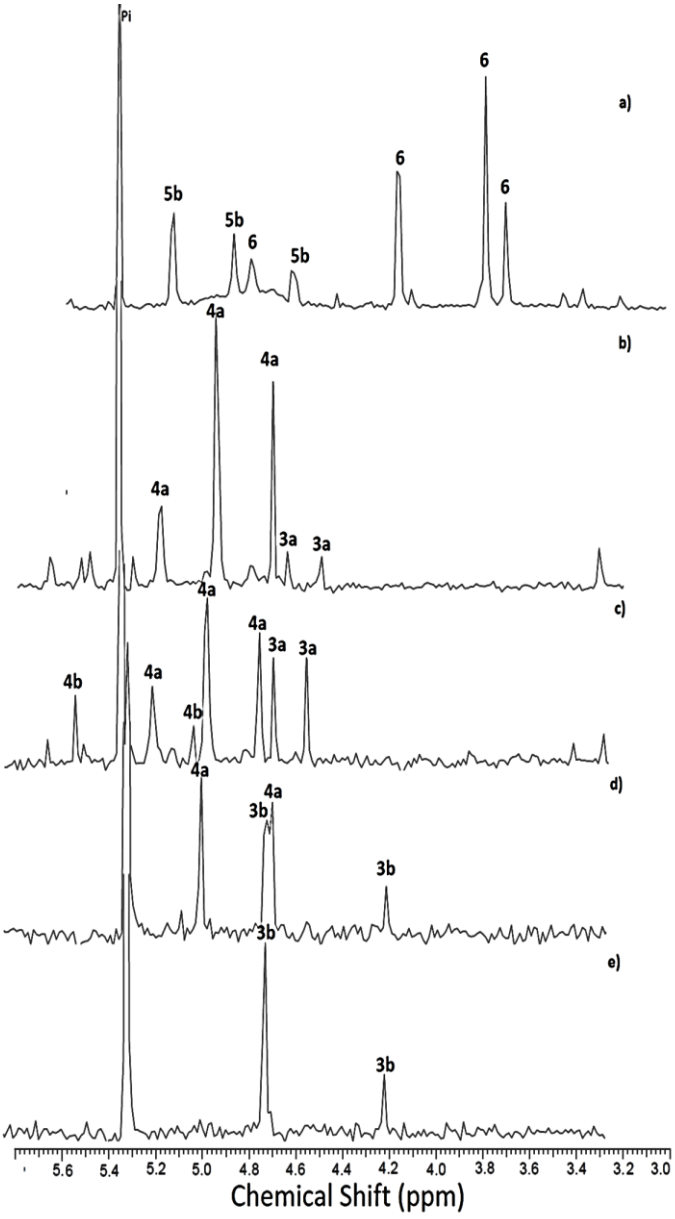

Fig 11. Progressive changes in ^{31}P NMR spectra during phytate degradation: a) 1.0 hr, b) 2.5 hrs, c) 4.2 hrs, d) 24.0 hrs, e) 48.0 hrs. Shift of each spectra was adjusted to orthophosphate peak shift as a reference. Symbols 6, 5, 4a, 4b, 3a, 3b used for peak identification correspond to IP_6, I(1,2,3,4,5)P_5, I(1,2,5,6)P_4, I(1,2,3,4) P_4/I(1,3,4,6) P_4, I(1,5,6) P_3 ,and I(1,2,3) P_3/(1,2,6) P_3 respectively.

after 1 hr and 4.2 hrs respectively with the peaks for IP_4 and IP_3 remaining after 24 hrs. This indicates that the degradation of IP_4 and IP_3 is much slower than that of IP_6 and IP_5. This delay could be attributed to a variety of reasons. For example, accumulation of phosphate inhibiting the reaction, decreased phytase activity in the solution or lower inositol phosphates being more recalcitrant to degradation. Minor fluctuation in peak shift for each successive time point could be due to changes in pH.

3.3.3 Comparison of ^{31}P NMR, $^{1}H-^{31}P$ NMR Spectroscopy and HPLC data

The ^{31}P NMR and HPLC results on the same degradation products enabled cross-comparison and cross-referencing for NMR peaks. The identity of degradation products and their percentage calculated by NMR analysis and HPLC results are compared in Table 3. The percentages are quite close for most of the products while the difference can be attributed to peak overlapping and incomplete peak assignment. The failure of detection of IP_2 and IP_1 in the samples might be due to complete degradation of IP_2, but the possibility of phytate being completely degraded to myo-inositol is ruled out because our enzyme was pure and the highest amount of degradation detected by colorimetric measurement was ~500% (Fig. 9). As shown in Table 3, both NMR and HPLC data show strong corroboration for the identity of various IP_x. In this study, only ^{31}P NMR and ^{1}H-^{31}P NMR spectra were generated and analyzed because of simplicity and high resolution of P and H peaks. However, for high resolution studies to resolving more ambiguous peaks, correlation spectroscopies (i.e. TOCSY, HNMR, and CNMR) could be utilized. In this study, model inositol compounds and HPLC measurements were sufficient to resolve peak identity solely through peak shift, peak area, and proton coupling parameters. The strong corroboration of NMR peaks to HPLC results points to the usefulness and reliability of utilizing NMR spectroscopy to non-destructively analyzing phytate and partially dephosphorylated inositol phosphates.

3.4. Oxygen Isotope Effects of Phytate Degradation

Given that phosphorus atoms in a phytate molecule remains as phosphate and one of the four oxygen atoms is covalently bonded to carbon (P−O−C bond), nucleophilic attack of the P−O−C ester and cleavage at the P−O bond position requires one oxygen atom to be

incorporated to the released phosphate from external ambient sources. During enzymatic hydrol ysis of P-monoester compounds, the sole O atom source is ambient water with the fractionation factors depending on the enzyme or substrate type (Liang and Blake, 2006a). Because the nucleophilic attack could be influenced by the nature of the groups adjacent to the P−O−C bond

Table 3. Comparison of NMR and HPLC results for phytate degradation products

Degradation Time (hr)		*Phytate degradation products*					
		Pi	***I(1,2,3,4,5,6)P_6***	***I(1,2,3,4,5)P_5***	***I(1,2,5,6)P_4***	***I(1,5,6)P_3***	***I(1,2,3)P_3***
1	Shift (ppm)	5.35	4.79,4.17,3.79,3.69	5.12,4.86,4.62			
	^{3}J(Hz)		11.89/9.9	11.89,7.83, 5.94			
	NMR (%)		66.2%	53.5%			
	HPIC (%) *		49.4%	50.6%			
2.5	Shift (ppm)	5.16			4.97,4.74,4.5	5.45,5.28, 3.1	
	^{3}J(Hz)				9.91,7.93,9.91	5.94, 7.93,7.93	
	NMR (%)				90.7%	9.3%	
	HPIC (%) *				80.4%	19.6%	
4.2	Shift (ppm)	5.16			4.93,4.68,4.45	5.04, 4.39, 4.24	
	^{3}J(Hz)				9.91,5.93,7.93	9.91,7.84/11.86,9 .91	
	NMR (%)				63.3%	36.7%	
	HPIC (%) *				57.9%	42.1%	
24	Shift (ppm)	5.06			4.74,4.46, N/A		4.44, 3.95
	^{3}J(Hz)				9.91,7.93, N/A		7.93
	NMR (%)				-----[a]		-----[a]
	HPIC (%) *				46.2%		65.3%
48	Shift (ppm)	5.06					4.46,3.95
	^{3}J(Hz)						7.93,7.93
	NMR (%)						-----[b]
	HPIC (%) *						-----[b]

[a] Peak overlap interfered with integration

[b] Only one species detected in ^{31}PNMR

* Adjusted to only species identified in the ^{31}PNMR

in the phytate and the six different PO_4 moieties in phytate could originally have different $\delta^{18}O_p$ values, phosphates released during successive degradation steps were individually processed and corresponding $\delta^{18}O_p$ values were measured. In order to detect whether O from water and air is incorporated into released Pi, and to infer reaction mechanisms, series of experiments are carried out in three different ^{18}O labeled air and seven different ^{18}O labeled waters.

^{18}O labeled air experimental results show no evidence of oxygen from air being incorporated to the released Pi (Fig. 12). Please note that if O from labeled air is incorporated in the released Pi, corresponding changes in the $\delta^{18}O_p$ values of released Pi should be observed. Experiments conducted with labeled air having $\delta^{18}O_{O2}$ value difference of more than 100‰ show that the $\delta^{18}O_p$ values of released Pi are quite similar as indicated by the almost zero slope (~1.0%, negligible slope) in the linear relationship of $\delta^{18}O_p$ values of Pi and $\delta^{18}O_{O2}$ values of O_2.

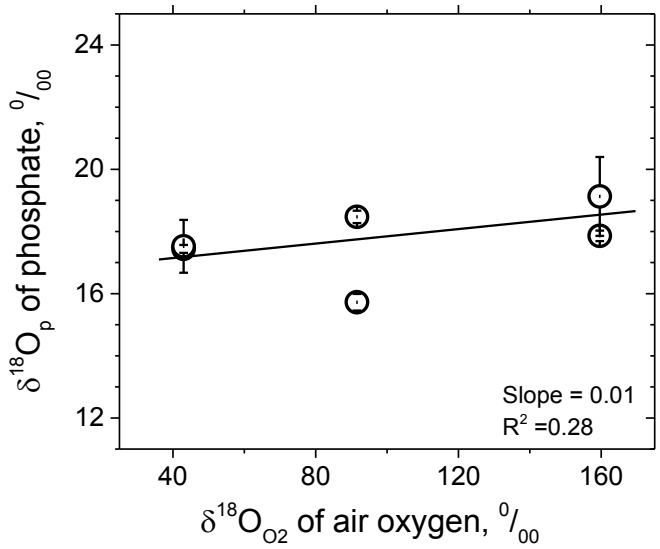

Fig 12. Plot of $\delta^{18}O_p$ of released Pi and $\delta^{18}O_{O2}$ values of labeled O_2 used in phytate degradation experiment. The slope of the linear regression is ~1%.

Results of phytate degradation experiments performed with ^{18}O labeled water are presented in Fig. 13 (a, b). Our data show that the $\delta^{18}O_p$ values of released Pi as a function of time (see Fig. 7 for the extent of degradation at different time points) i.e., during successive degradation of phytate and releasing PO_4 from different positions in the inositol ring remained unchanged (Fig. 13a). This is a unique observation that suggests that the different PO_4 moieties

in phytate have the same original isotopic compositions (i.e., same $\delta^{18}O_{PO}$ values). This result relieves the need to completely degrade phytate to characterize its isotopic composition.

The incorporation of oxygen atom from ambient water during the release of Pi is evidenced in the corresponding changes in $\delta^{18}O_p$ values of released Pi in the experiments performed in ^{18}O labeled waters (Fig. 13 b). Please note that the $\delta^{18}O_w$ values of water were varied from –6.91 to 73.55 ‰ in these experiments. The regression of $\delta^{18}O_w$ values of water and the $\delta^{18}O_P$ values of the released Pi show a linear relationship with a slope of 0.23 (Fig. 13b). This slope indicates the proportions of ambient water incorporated in the released Pi, thus suggesting that ~25% (or one out of four) oxygen atoms in the released Pi are incorporated from the ambient water during the phytate degradation. This also means that 75% of oxygen atoms (i.e., three out of the four oxygen atoms) were inherited from original phytate substrate ($\delta^{18}O_{PO}$). Overall, this result verifies that the nucleophilic attack is solely caused by water and the cleavage of P−O−C ester during phytate degradation incorporates oxygen solely from ambient water in the released Pi.

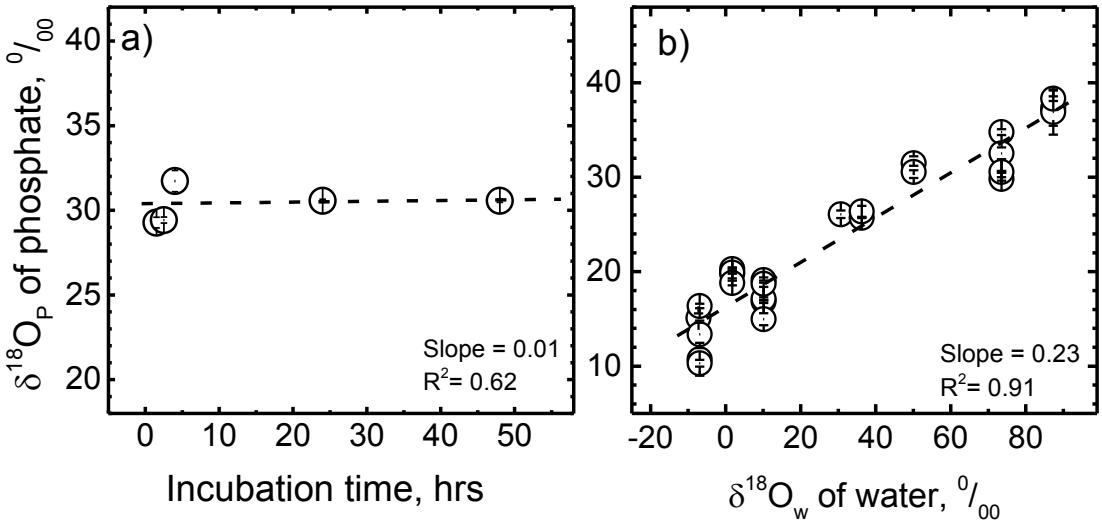

Fig. 13. a) Changes in $\delta^{18}O_p$ values of the released Pi as a function of increasing extent of phytate degradation. $\delta^{18}O_w$ value of the ^{18}O labeled water used in the experiment was 73.55 ‰. b) $\delta^{18}O_p$ value of released Pi in different ^{18}O labeled waters.

Oxygen atom incorporated into Pi during P_o hydrolysis is accompanied by the fractionation relative to the ambient water oxygen (Liang and Blake, 2006a; 2009). The knowledge of $\delta^{18}O_{PO}$ value of original PO_4 moieties in the phytate is necessary to determine the fractionation factor. Given that phytate has six PO_4 moieties and other sources of oxygen is quite low (O as -OH can vary from 4−6 depending on the pH) compared to that of 24 Os from phosphate, highly acidic form of phytate (pH 2.1) was directly analyzed in the isotope mass spectrometer to obtain $\delta^{18}O_{PO}$ values of the organically bound PO_4. At this pH number of other structural Os in the phytate could be ≤1. The measured $\delta^{18}O_{PO}$ values of phytate was 19.9 ‰. Based on the original $\delta^{18}O_{PO}$ values of phytate, $\delta^{18}O_P$ values of released Pi, and $\delta^{18}O_w$ values ambient waters, fractionation factors of water (between ambient and incorporated in P_i) were calculated using the equation previously established by Liang and Blake (2006a) as follows:

$$F = 4 \times \left[\delta^{18}O_P - 0.75\delta^{18}O_{PO}\ \right] - \ \delta^{18}O_w \qquad \text{(ii)}$$

The fractionation factors varied from –42 to +24 ‰ with average value of +1(±16). It means both ^{16}O and ^{18}O are preferentially incorporated to the released P_i. It is unclear what causes such large ranges of fractionation factors. Potential causes could be that 6' phytase and 3' phytase acting in concert but at different extents at different times or the activity of any other unknown phosphatases, if present, in the purified phytase. Since the fractionation factors depend on the enzyme reaction kinetics and given that the rates of dephosphorylation of different IPx varied significantly (see HPLC results above), variable fractionation factors may be the reflection of different reaction times. The reason that a wide range of fractionation factors not found in other monoesters (Liang and Blake, 2006a; Sandy et al., 2013; von Sperber et al., 2014) may be due to the presence of single PO_4 moiety in the monoesters studied in the past and relatively straightforward degradation mechanism involving one enzyme and one substrate with one phosphate moiety on them. Future research is needed to identify the wide range of fractionation factors. Positive fractionation factors during phytate degradation, however, could provide a unique signature of Pi derived from phytate. This could further be used to distinguish Pi source of phytate with other phosphomonoesters and possibly other P_o compounds.

3.5 Phosphatase Enzymes and Mechanisms of Nucleophilic Attack by Wheat Phytase

There are four different classes of phosphatases that are known to have phytase activity: histidine acid phosphatase (HAP), β-Propeller phytase (BPP), cysteine phosphatase (CP), and purple acid phosphatase (PAP) (Mullaney and Ullah, 2007). Among which HAP and PAP are known to exist in wheat phytase (Rasmussen et al., 2007; Dionisio et al, 2011). HAP covers a large class of enzymes that are commonly present in animals, plants and microorganisms (Mullaney and Ullah, 2007) and share a common catalytic mechanism. The suggested catalytic mechanism of HAP is that the histidine residue in the enzyme serves as a nucleophile during the reaction and forms a covalent phosphohistidine intermediate while the acid residue of enzyme functions as a proton donor to the oxygen atom of the phosphomonoester bond (Oh et al., 2004).

The phosphatase targeted in the purification process in this study was PAP (that has molecular weight of ~60 kDa). Presence of PAP was indirectly confirmed by the protein band of SDS gel electrophoresis (data not shown), but the existence of other phosphatase could not be ruled out. All PAPs are also considered to employ a similar catalytic mechanism for hydrolysis of monophosphate ester bonds (Schenk et al., 2013). The proposed catalytic mechanism (Fig. 14) shows that substrate initially binds to the PAP to form a pre-catalytic complex and is followed by the coordination of substrate with metal ions in the active site, which facilitates the nucleophilic attack by a solvent-derived hydroxide (-OH from water in this study). Subsequently, esterolysis of the phosphomonoester leads to the breakage of the O–R bond in the P–O–R ester and release of leaving group while phosphate remains bound to the active site of the PAP. The regeneration of the resting state of enzyme requires the reformation of the hydroxide bridge on the enzyme and removal of phosphate group, which ultimately involves one oxygen atom from the water to the released Pi. This proposed catalytic mechanism strongly suggests that the generation of Pi by phytase incorporated one oxygen atom from the ambient water, which agrees well with the results from ^{18}O labeled air and water phytate degradation experiments. The formation and re-formation of hydroxide bridge and removal of phosphate group could delay the nucleophilic attack by –OH group and this also may vary due to positional difference of PO_4 moieties in phytate and in partially dephosphorylated inositol phosphates as well as in their corresponding stereoisomers. All of these factors may compound the enzymatic degradation rates and result in variable fractionation factors.

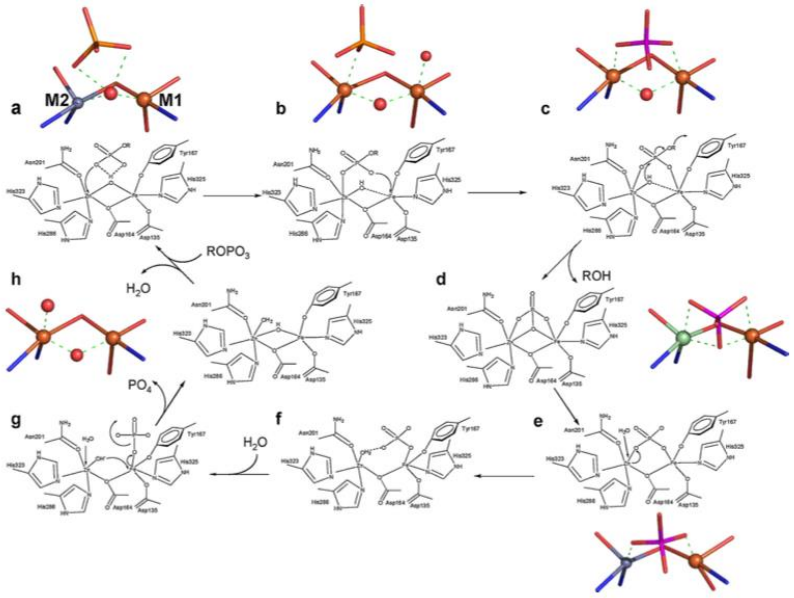

Fig 14. PAP-catalyzed phosphomonoester hydrolysis (reproduced from Schenk et al., 2013).

Chapter 4

CONCULUSIONS AND IMPLICATIONS

Large amounts of phytate and partially dephosphorylated products exist in soils as well as in aquatic systems while the origins, chemical forms, bioavailability, and mobility of these compounds in the environment are not well understood (Turner et al., 2007, Giles and Cade-Menun, 2014). With increasing phytate P in agricultural soils due to manure application and consequential increase in environmental concern due to elevated P in many open waters, development of new methods that have higher specificity to elucidate the mechanisms and pathways of inositol phosphate degradation as well as capability for tracking sources of dissolved P has been an ever more pressing needs. In fact, the source identity of P in open waters has not been addressed in the past because of the inability, based on concentration alone, to determine P sources. This means that once P from a distinct source is released to the environment and different sources mix with each other, the origin and history of P are largely lost.

Application of stable isotopes to understand inositol phosphate degradation is rare while the application of phosphate oxygen isotope ratios is non-existent, and there have not been previous attempts made to understand the oxygen isotopic fractionation during stepwise degradation of organophosphorus compounds. Isotope research has the great potential to advance our understanding of degradation mechanisms of organophosphorus compounds by linking specific degradation pathways with isotope effects, so that the source of P_i released from inositol phosphate or other organophosphorus compounds can be identified. Research results show that the cleavage of P–O bonds during inositol phosphate degradation is accompanied by the introduction of one oxygen atom solely from water to the released P_i. The oxygen fractionation factors between ambient and incorporated waters varied highly (-42 to +24 ‰). It is unclear what causes such large ranges of fractionation factors, but it is speculated that it is due to the presence of both 6’ phytase and 3’ phytase in the purified phytase, formation and reformation of the hydroxide bridge, and removal of a phosphate group during nucleophilic attack by an –OH group in the PAP enzyme and various rates of degradation of partially degraded products and different isomers. Positive fractionation factors during inositol phosphate degradation, yet unknown for all

monoesters studied so far, could provide a unique signature of P_i derived from inositol phosphate. This could further be used to distinguish sources of P_i to inositol phosphate and other phosphomonoesters. Furthermore kinetics and pathways of enzymatic inositol phosphate degradation by using NMR and HPLC provided better constrained degradation pathways that included a previously identified and a new pathway of inositol phosphate degradation. The consistency of the results from NMR and HPLC methods demonstrated the promising combination of these two techniques to study the inositol phosphate degradation kinetics and pathways.

Specific linkage of the enzymatic degradation pathways with oxygen isotope effects could lend support to the application of this tool to the degradation of inositol phosphate in the environment while NMR and HPLC could be used to identify the degradation pathway. However, the current state of research that shows linkage between reaction mechanism and isotopic fractionation is limited and thus the generalization for other organic phosphorus compound degradation cannot be made. Overall, research aimed at understanding of biogeochemical cycling of inositol phosphate, particularly the source and pathway of its degradation in the environment could, in the long term, promote the development of a sustainable P management strategy in agricultural systems with respect to minimizing the use of mineral fertilizers by increasing the availability of inositol phosphate to plants and, in consequence, ultimately reduce potential P loss from agricultural systems to surface and subsurface waters.

REFERENCES

Adeola O., Sands J.S., Simmins P.H. and Schulze H. (2004) The efficacy of an *Escherichia. coli*-derived phytase preparation. *J. Anim. Sci.* **82**, 2657-2666.

Anderson G. (1980) Assessing organic phosphorus in soil. In *The role of phosphorus in agriculture* (ed. F. E. Khasawneh, E. C. Sample and E. J. Kamprath). American Society of Agronomy, Madison, USA, pp. 411-431.

Bassiri A. and Nahapetian A. (1977) Differences in concentrations and interrelationships of phytate, phosphorus, magnesium,calcium, zinc and iron in wheat varieties grown under dryland and irrigated conditions. *J. Agric. Food Chem*. **25**, 1118.

Benitez-Nelson C.R. (2000) The biological cycling of phosphorous in marine systems. *Earth Sci. Rev.* **51**, 109-135.

Blake R. E., O'Neil J. R. and Garcia G. A. (1997) Oxygen isotope systematics of microbially mediated reactions of phosphate: I. Degradation of organophosphorus compounds. *Geochim. Cosmochim. Acta* **61**, 4411-4422.

Blake R.E., O'Neil J.R. and Garcia G. A. (1998) Effects of microbial activity on the d18OP of dissolved inorganic phosphate and textural features of synthetic apatite. *Am. Mineral*. **83**, 1516-1531.

Braun A M, Frimmel F. H, and Haigne J (1986) Singlet oxygen analysis in irradiated surface waters. *Int J Environ Anal Chem* 27, 137–149

Brejnholt S.M, Dionisio G., Glitsoe V., Skov L. K. and Brinch-Pedersen H. (2010) The degradation of phytate by microbial and wheat phytases is dependent on the phytate matrix and the phytase origin. *J. Sci. Food Agric*. **91**, 1398-1405.

Cade-Menun B. and Liu C. (2013). Solution phoshporus-31 nuclear magnetic resonance spectroscopy of soils from 2005 to 2013: A review of sample preparation and experimental parameters. *Soil Sci. Soc. Am. J.* **78**, 19-37.

Cade-Menun B.J. (2005) Characterizing phosphorus in environmental and agricultural samples by 31P nuclear magnetic resonance spectroscopy. *Talanta.* **66**, 350-371.

Casals I., Villar J. L. and Riera-Codina M. (2002) A straightforward method for analysis of highly phosphorylated inositols in blood cells by high-performance liquid chromatography. *Anal. Biochem.* **300**, 69-76.

Celi L. and Barberis E. (2007) Abiotic reactions of inositol phosphates in soil. In *Inositol Phosphates Linking Agriculture and the Environment* (ed. Turner B. L., Richardson A. E., and Mullaney E. J.). CAB International, Oxford, UK, pp. 207-220.

Celi L., Lamacchia S. and Barberis E. (2000) Interaction of inositol phosphate with calcite. *Nutr. Cycl. Agroecosys*. **57**, 271-277.

Chen Q.C. and Li B.W. (2003) Separation of phytic acid and other related inositol phosphates by high-performance ion chromatography and its applications. *J. Chromatogr*. **1018**, 41-52.

Chester T.L. (2013) Recent developments in high-performance liquid chromatography stationary phases. *Anal. Chem*. **85**, 579-589.

Clark L.L., Ingall E.D. and Benner R. (1999) Marine organic phosphorus cycling: novel insights from nuclear magnetic resonance. *Am. J. Sci.* **299**, 724-737.

Cooper W.T., Heerboth M. and Salters V.J.M. (2007) High-perfomance chromatographic separations of inositol phosphates and their detection by mass spectrometry. In *Inositol Phosphates Linking Agriculture and the Environment* (ed. Turner B. L., Richardson A. E., and Mullaney E. J.). CAB International, Oxford, UK, pp. 207-220.

Cottrill M.A., Golovan S.P., Philips J.P., and Forsberg C.W. (2002). Inositol phosphatase activity in E. coli agp-encoded acid glucose-1-phosphatase, *Can. J. Microbiol*. **48**, 801-809.

Dionisio G et al. (2011). Cloning and characterization of purple acid phosphatase phytases from wheat, barley, maize, and rice. *Plant Physiol.* **156**, 1087-1100.

Fredrikson M., Andlid T., Haikara A. and Sandgerg A.-S. (2002) Phytate degradation by micro-organisms in synthetic media and pea flour. *J. Appl. Microbiol*. **93**, 197-204.

Greiner R. (2004) Degradation of *myo*-inositol hexakisphosphate by a phytate-degrading enzyme from *Pantoea agglomerans. Protein J.* **23**, 577-585.

Greiner R. (2007) Phytate degrading enzymes: Regulation of synthesis in microorganisms and plants In *Inositol Phosphates Linking Agriculture and the Environment* (ed. Turner B. L., Richardson A. E., and Mullaney E. J.). CAB International, Oxford, UK, pp.78-92.

Greiner R. and Larsson Alminger M. (2001) Stereospecificity of *myo*-inositol hexakisphosphate dephosphorylation by phytate-degrading enzymes of cereals. *J. Food Biochem.* **25**, 229-248.

Greiner R., Carlsson N.G. and Larsson Alminger M. (2000) Stereospecificity of *myo-inositol* hexakisphosphate dephosphorylation by a phytate-degrading enzyme of *Escherichia coli. J. Biotechnol.* **84**, 53-62.

Greiner R., Farouk A., Larsson Alminger M. and Carlsson, N. (2002) The pathway of dephosphorylation of *myo*-inositol hexakisphosphate by phytate-degrading enzymes of different *Bacillus* spp. *Can. J. Microbiol.* **48**, 986-994.

Greiner R., Haller E., Konietzny U. and Jany K.D. (1997) Purification and characterization of a phytase from *Klebsiella terrigena. Arch. Biochem. Biophys.* **341**, 201-206.

Greiner R., Haller E., Konietzny U. and Jany, K. -D. (1997) Purification and characterization of a phytase from *Klebsiella terrigena. Arch. Biochem. Biophys.* **341**, 201-206.

Greiner R., Konietzny U. and Jany, K. -D. (1993) Purification and characterization of two phytases from *Escherichia coli. Arch. Biochem. Biophys.* **303**, 107-113.

Haefner S., Knietsch A., Scholten E., Braun J., Lohscheidt M., Zelder O. (2005) Biotechnological production and application of phytases. *Appl. Microbiol. Biotechnol.* **68**, 588-597.

Harland B.F., Smike-Williams S. and Oberleas D. (2004) High performance liquid chromatography analysis of phytate (IP6) in selected foods. *J. Food Comp. Anal.* **17**, 227-233.

Hill J.E. and Richardson A.E. (2007) Isolation and assessment of microorganisms that utilize phytate. In *Inositol Phosphates Linking Agriculture and the Environment* (ed. Turner B. L., Richardson A. E., and Mullaney E. J.). CAB International, Oxford, UK, pp. 207-220.

Hoffman (2013) ^{31}P NMR. Retrieved on 07/03/2014 from http://chem.ch.huji.ac.il/nmr/techniques/1d/row3/p.html

International Union of Pure and Applied Chemistry (1971) *Nomenclature of inorganic chemistry, definitive rules 1970.* Butterworths, London.

Jaisi D.P, Blake R.E. , Kukkadapu R.K. (2010) Fractionation of oxygen isotopes in phosphate during its interactions with iron oxides. *Geochim Cosmochim Acta* **74**, 1309–1319.

Jaisi D.P., Blake R.E. (2010) Tracing sources and cycling of phosphorus in Peru Margin sediments using oxygen isotopes in authigenic and detrital phosphates. *Geochim. Cosmochim. Acta* **74**, 3199-3212.

Jaisi D.P. and Blake R. (2014) Advances in using oxygen isotope ratios of phosphate to understand phosphorus cycling in the environment. In *Advances in Agronomy* (ed. Sparks D.L.). Elsevier Science. Burlington. pp. 1-38.

Jaisi D.P., Blake R., Liang, Y. and Chang S. (2014) Investigation of compound-specific organic-

inorganic phosphorus transformation using stable isotope ratios in phosphate. In *Applied Manure and Nutrient Chemistry for Sustainable Agriculture and Environment* (ed. He Z. and Zhang H.) Dordrecht: Springer. pp. 267-292.

Johnson B.B., Quill E. and Angove M.J. (2012) An investigation of the mode of sorption of inositol hexaphosphate to goethite. *J. Colloid Interface Sci.* **367**, 436-442.

Kemme P.A., Lommen A., De Jonge L.H., Van der Klis J.D., Jongbloed A.W., Mroz Z. and Beynen A.C. (1999) Quantification of inositol phosphates using ^{31}P nuclear magnetic resonance spectroscopy in animal nutrition. *J. Agric. Food Chem.* **47**, 5116-5121.

Kerovuo, J., Rouvinen, J. and Hatzack, F. (2000) Hydrolysis of phytic acid by *Bacillus* phytase. *Biochem. J.* **352**, 623-628.

Konietzny U. and Greiner R. (2002) Molecular and catalytic properties of phytase-degrading enzymes (phytases). *Int. J. Food sci. Tech.* **37**, 791-812.

Konietzny, U. and Greiner, R. (2004) Bacterial phytase: potential application, *in vivo* function and regulation of its synthesis. *Braz. J. Microbiol.* **35**, 11-18.

Lassila J.K., Zalatan J.G. and Herschlag D.L. (2011) Biological phosphoryl-transfer reactions: understanding mechanism and catalysis. *Annu. Rev. Biochem*. **80**, 669-702.

Liang Y. and Blake R.E. (2006a) Oxygen isotope signature of P-I regeneration from organic compounds by phospho-monoesterases and photo-oxidation. *Geochim. Cosmochim. Acta* **70**, 3957-3969.

Liang Y. and Blake R.E. (2006b) Oxygen isotope composition of phosphate in organic compounds: isotope effects of extraction methods. *Org. Geochem*. **37**, 1263-1277.

Liang Y. and Blake R.E. (2009) Compound and enzyme-specific phosphate hydrolysis mechanisms revealed by δ^{18}O of dissolved phosphate, *Geochim. Cosmochim. Acta* **73**, 3782-3794.

Lindsay S. (1992) High performance liquid chromatography. Thames Polytechnic, London, UK.

Lipok J., Wieczorek D., Jewgin´ ski M., Kafarski P. (2009). Prospects of in vivo ^{31}P NMR method in glyphosate degradation studies in whole cell system. *Enzyme Microb. Technol*. **44**, 11-16.

Lung S.C. and Lim B.L. (2006) Assimilation of phytate-phosphorus by the extracellular phytase activity of tobacco (*Nicotiana tabacum*) is affected by the availability of soluble phytate. *Plant Soil* **279**, 187-199.

Maenz D.D. and Classen H.L. (1998) Phytase activity in the small intestinal brush border membrane of the chicken. *Poultry Sci.***77**, 557-563.

Meek J. L. and Nicoletti F. (1986) Detection of inositol triphosphate and other organic phosphates by high-performance liquid chromatography using an enzyme-loaded postcolumn reactor. *J. Chromatogr.* **351**, 303-311.

Miller, J. (1972). Experiments in Molecular Genetics. Cold Spring Harbor, NY: Cold Spring Harbor Laboratory.

Mullaney E.J. and Ullah A.H. (2003) The term phytase comprises several different classes of enzymes. *Biochem. Biophys. Res. Commun.* **312**, 179-184.

Mullaney E.J. and Ullah A.H. (2007) Phytases: Attributes, catalytic mechanisms and applications. In *Inositol Phosphates Linking Agriculture and the Environment* (ed. Turner B. L., Richardson A. E., and Mullaney E. J.). CAB International, Oxford, UK, pp.78-92.

Murphy J. and Riley I.P. (1962) A modified single solution method for the determination of phosphate in natural waters. *Anal. Chim. Acta* **27**, 31-36.

Murthy P.N. (2007) Identification of Inositol Phosphates by Nuclear Magnetic Resonance Spectroscopy: Unravelling Structural Diversity. In *Inositol Phosphates Linking Agriculture and the Environment* (ed. Turner B. L., Richardson A. E., and Mullaney E. J.). CAB International, Oxford, UK, pp.78-92.

Nakano T., Joh T., Narita K. and Hayakawa T. (2000) The pathway of dephosphorylation of *myo-inositol* hexakisphosphate by phytases from wheat bran of *Triticum aestivum* L. cv. nourin #61. *Biosci., Biotechnol., Biochem.* **64**, 995-1003.

Nanny M.A. and Minear R.A. (1994) Organic phosphorus in the hydrosphere. Characterization via ^{31}P Fourier transform nuclear magnetic resonance spectroscopy. In *Environmental chemistry of lakes and reservoirs* (ed. L. A. Baker), American Chemical Society, Washington, DC, pp.161-191.

Ognalaga M., Frossard E., Thomas F. (1994) Glucose-1-phosphate and myo-inositol hexaphosphate adsorption mechanisms on goethite. *Soil Sci. Soc. Am. J.* **58**, 332-337.

Oh, B.C., Choi, W.C., Park, S., Kim, Y.O. and Oh, T.K. (2004) Biochemical properties and substrate specificities of alkaline and histidine acid phytases. *Appl. Microbiol. Biotechnol.* **63**, 362-372.

Raboy V. (2003) *Myo*-inositol-1,2,3,4,5,6-hexakisphosphate. *Phytochemistry* **64**: 1033-1043.

Rasmussen S., Sorensen M.B and Johansen K.S. (2007) Polynucleotides encoding phytase polypeptides. U.S. Patent.

Sandberg A.-S., Rossander H.L. and Türk, M. (1996) Dietary *Aspergillus niger* phytase increases iron absorption in humans. *J. Nutr.* **126,** 476-480.

Sandy, E., Yao, J., Blake, R.E. (2013) Isotope effect of phytate and phosphonate mineralization. *J. Haz. Mat*. **260**, 947-954.

Schenk G., Mitic´N. Hanson G. R. and Comba P. (2013) Purple acid phosphatase: A journey into the function and mechanism of a colorful enzyme. *Coord. Chem. Rev*. **257**, 473-482.

Shan Y., McKelvie I. D. and Hart B. T. (1993) Characterization of immobilized *Escherichia coli* alkaline phosphatase reactors in flow injection analysis. *Anal. Chem.* **65,** 3053-3060.

Shang C., Huang P.M. and Stewart J.W.B. (1990) Kinetics of adsorption of organic and inorganic phosphates by short-range ordered precipitate of aluminum. *Can. J. Soil Sci.* **70**, 46l-470.

Shears S.B. and Turner B. L. (2007) Nomenclature and Terminology of Inositol Phosphates: Clarification and a Glossary of Terms In *Inositol Phosphates Linking Agriculture and the Environment* (ed. Turner B. L., Richardson A. E., and Mullaney E. J.). CAB International, Oxford, UK, pp.1-6.

Thayer J.R., McCormick R.M. and Advalovic N. (1996) High-resolution nucleic acid separations by high-performance liquid chromatography. *Method Enzymol.* **271**, 147-174.

Touati E., Dassa E., Dassa J. and Boquet P.L. (1987) Acid phosphatase (pH 2.5) of *Escherichia coli:* regulatory characteristics. In *Phosphate Metabolism and Cellular Regulation in Microorganisms.* (ed. Torriani-Gorini, A., Rothman, F.G., Silver, S., Wright, A. and Yagil, E.) American Society for Microbiology, Washington, DC, pp. 31-40.

Turner B.L., Lambin E. F. and Reenberg A. (2007) The emergence of land change science for global environmental change and sustainability. *Proc. Natl. Acad. Sci.***104**, 20666-20671.

Turner B.L., Mahieu N. and Condron L.M. (2003) Quantification of *myo*-inositol hexakisphosphate in alkaline soil extracts by solution ^{31}P NMR spectroscopy and spectral deconvolution. *Soil Sci*. **168**, 469-478.

Turner B.L., Paphazy M., Haygarth P.M. and McKelvie I.D. (2002) Inositol phosphates in the environment. *Philos. Trans. R. Soc. Lond.* B **357**, 449-469.

van der Kaay J. and van Haastert J.M. (1995) Stereospeficity of inositol hexakisphosphate

dephosphorylation by *Paamecium* phytase. *Biochem. J.* **312**, 907-910.

Vennemann T.W., Fricke H.C., Blake R.E., O'Neil J.R., Colman A.. (2002) Oxygen isotope analysis of phosphates: a comparison of techniques for analysis of Ag_3PO_4 , *Chem. Geol.* **185**, 321–336.

von Sperber C., Kries H., Tamburini F., Bernasconi S.M. and Frossard E. (2014) The effect of phosphomonoesterases on the oxygen isotope composition of phosphate. *Geochim. Cosmochim. Acta* **125**, 519-527.

Williams S.G. (1970) The role of phytic acid in the wheat grain. *Plant Physiol*. **45**, 376-381.

Yi Z. and Kornegay E.T. (1996). Sites of phytase activity in the gastrointestinal tract of young pigs. *Anim. Feed Sci. Technol*. **61**, 261-268.

Zhang Y.S., Werner W., Scherer H.W. and Sun X. (1994) Effect of organic manure on organic phosphorus fractionation in two paddy soils. *Biol. Fertil. Soils* **17**, 64-68.